

EFFECTS OF 3D PRINTER PARAMETERS ON CONDUCTIVITY OF NANO-TITANIUM
DIOXIDE ON ELECTRODE SOLAR CELLS



A Dissertation Submitted in Partial Fulfillment of the Requirements
for the Degree of Doctor of Philosophy in Imaging Technology
Department of Imaging and Printing Technology
FACULTY OF SCIENCE
Chulalongkorn University
Academic Year 2019
Copyright of Chulalongkorn University

ผลของพารามิเตอร์เครื่องพิมพ์แบบสามมิติต่อการนำไฟฟ้าของนาโนไททาเนียมไดออกไซด์บน
ขั้วไฟฟ้าสำหรับเซลล์สุริยะ



วิทยานิพนธ์นี้เป็นส่วนหนึ่งของการศึกษาตามหลักสูตรปริญญาวิทยาศาสตรดุษฎีบัณฑิต
สาขาวิชาเทคโนโลยีทางภาพ ภาควิชาเทคโนโลยีทางภาพและการพิมพ์
คณะวิทยาศาสตร์ จุฬาลงกรณ์มหาวิทยาลัย
ปีการศึกษา 2562
ลิขสิทธิ์ของจุฬาลงกรณ์มหาวิทยาลัย

Thesis Title	EFFECTS OF 3D PRINTER PARAMETERS ON CONDUCTIVITY OF NANO-TITANIUM DIOXIDE ON ELECTRODE SOLAR CELLS
By	Mr. Krairop Charoensopa
Field of Study	Imaging Technology
Thesis Advisor	Associate Professor ARAN HANSUEBSAI, Ph.D.
Thesis Co Advisor	Associate Professor Kazuhiro Manseki, Ph.D.

Accepted by the FACULTY OF SCIENCE, Chulalongkorn University in Partial
Fulfillment of the Requirement for the Doctor of Philosophy

..... Dean of the FACULTY OF SCIENCE
(Professor POLKIT SANGVANICH, Ph.D.)

DISSERTATION COMMITTEE

..... Chairman
(Associate Professor Pontawee Pungrassamee)

..... Thesis Advisor
(Associate Professor ARAN HANSUEBSAI, Ph.D.)

..... Thesis Co-Advisor
(Associate Professor Kazuhiro Manseki, Ph.D.)

..... Examiner
(Assistant Professor CHAWAN KOOPIPAT, Ph.D.)

..... Examiner
(Associate Professor PICHAYADA KATEMAKE, Ph.D.)

..... External Examiner
(Assistant Professor Panitat Hasin, Ph.D.)

ไกรพ เจริญโสภา : ผลของพารามิเตอร์เครื่องพิมพ์แบบสามมิติต่อการนำไฟฟ้าของนาโนไททาเนียมไดออกไซด์บนขั้วไฟฟ้าสำหรับเซลล์สุริยะ. (EFFECTS OF 3D PRINTER PARAMETERS ON CONDUCTIVITY OF NANO-TITANIUM DIOXIDE ON ELECTRODE SOLAR CELLS) อ.ที่ปรึกษาหลัก : รศ. ดร.อรุณ หาญสีบสาย, อ.ที่ปรึกษาร่วม : รศ. ดร.คาซูฮิโร แมนซากิ

การประกอบขึ้นรูปสารนำไฟฟ้าบนอิเล็กโทรดของอุปกรณ์อิเล็กทรอนิกส์ด้วยเทคนิคการพิมพ์ เริ่มได้รับความนิยมนำไปใช้โดยเฉพาะเทคโนโลยีการพิมพ์สามมิติแบบขึ้นรูปด้วยวัสดุเหลว หรือที่เรียกว่า Liquid Deposition Modelling (LDM) กำลังได้รับความสนใจในอุตสาหกรรมอิเล็กทรอนิกส์ งานวิจัยนี้ได้ประยุกต์นำเทคโนโลยีสามมิติแบบ LDM ไปใช้ผลิตเซลล์สุริยะชนิดสีย้อมไวแสง (Dye Sensitized Solar Cell, DSSC) ด้วยการประกอบขึ้นรูปฟิล์มบางนาโนไททาเนียมไดออกไซด์ (TiO_2) บนแผ่นอิเล็กโทรดหรือขั้วไฟฟ้าแอโนด ศึกษาผลของพารามิเตอร์ในการตั้งเครื่องพิมพ์สามมิติได้แก่ ขนาดหัวพ่น (nozzle) ความเร็วในการพิมพ์ แรงดันลม และระยะหัวพ่นกับผิวอิเล็กโทรด ต่อคุณภาพของฟิล์มบาง TiO_2 และค่าความต้านทานการนำไฟฟ้า เพื่อให้สามารถนำไปใช้ผลิตเซลล์สุริยะชนิดสีย้อมไวแสงต่อไปได้ การทดลองนี้เริ่มด้วยการนำสาร nano- TiO_2 PST-18NR (P25) สำเร็จรูป ไปหาอัตราส่วนที่เหมาะสมกับสารละลายเอทานอล 99.5% วัดค่าการไหลของสารตัวอย่าง ทำการทดสอบพิมพ์ด้วยการตั้งค่าพารามิเตอร์ของเครื่องพิมพ์ที่ต่าง ๆ กัน นำแผ่นชั้นฟิล์มบางที่ได้ไปอบที่อุณหภูมิ 500 องศาเซลเซียส ทำการวิเคราะห์หาความสม่ำเสมอ ความหนา ความหยาบของผิว ภาวะแตก (cracking) และค่าความต้านทานการนำไฟฟ้า ของแผ่นตัวอย่างที่ประกอบขึ้นรูป ผลการทดลองพบว่า สมบัติสภาพการไหลของสาร TiO_2 มีผลต่อการตั้งค่าพารามิเตอร์ของเครื่องพิมพ์ ที่จะทำให้เกิดแรงในการพ่นสาร TiO_2 อยู่ในปริมาณที่เหมาะสม ได้ความหนาของชั้นฟิล์มที่คุณภาพดีและไม่เกิดการแตก ให้ค่าความต้านทานการนำไฟฟ้าระหว่าง $5.10 - 5.77 \text{ M}\Omega/\text{Sq.}$ และนำไปขึ้นรูปเป็นเซลล์ DSSC ได้ สภาวะการพิมพ์นี้ยังมีข้อจำกัดที่ได้ความหนาเพียง $6 \pm 0.25 \mu\text{m}$ และการพิมพ์หลายชั้นไม่มีผลต่อการเพิ่มความหนาของชั้นฟิล์มอย่างมีนัยสำคัญ ให้ค่าประสิทธิภาพของการเปลี่ยนพลังงานแสงอาทิตย์เป็นพลังงานไฟฟ้า 4 % ที่น่าสนใจคือ การศึกษาที่มีความเป็นไปได้ในการออกแบบชั้นฟิล์มให้มีรูปร่างต่าง ๆ เมื่อนำไปประกอบขึ้นเป็น DSSCs วัดค่าประสิทธิภาพของการเปลี่ยนพลังงานแสงอาทิตย์เป็นพลังงานไฟฟ้าได้ที่ค่าเฉลี่ย 3%

สาขาวิชา เทคโนโลยีทางภาพ
ปีการศึกษา 2562

ลายมือชื่อนิสิต
ลายมือชื่อ อ.ที่ปรึกษาหลัก
ลายมือชื่อ อ.ที่ปรึกษาร่วม

5872861023 : MAJOR IMAGING TECHNOLOGY

KEYWORD: 3D printing, Dye Sensitized Solar Cell, Nano-Titanium dioxide, LDM

Krairop Charoensopa : EFFECTS OF 3D PRINTER PARAMETERS ON CONDUCTIVITY OF NANO-TITANIUM DIOXIDE ON ELECTRODE SOLAR CELLS. Advisor: Assoc. Prof. ARAN HANSUEBSAI, Ph.D. Co-advisor: Assoc. Prof. Kazuhiro Manseki, Ph.D.

Fabricating conductive materials on electrode of electronic devices with printing techniques continues to gain popularity, including 3D printing especially Liquid Deposition Modelling (LDM) technology which is being interested in electronics industry. This research applied LDM 3D printing to fabricate nano-Titanium dioxide (TiO_2) thin film on an electrode or anode. The aim of research was to study the effect of parameters for setting the printer, such as nozzle size, printing speed, air pressure and nozzle distance from the electrode surface, on the quality of TiO_2 thin film and related sheet resistance. The experiment began with the paste samples preparation by mixing between the ready-made nano- TiO_2 PST-18NR (P25) with ethanol 99.5% and the flow of each paste was considered. Then a printing test was performed by adjusting the combination of the variation of the printer parameters. The obtained wet thin films were annealed in a chamber at temperature of 500 degree Celsius for 4 hours. The dried thin films' characteristics were analyzed by evaluating uniformity, thickness, roughness, cracking and sheet resistance which led to achieve good quality electrode. The results showed that the rheology of TiO_2 paste sample was important to set the printer parameters to give the proper force to extrude the TiO_2 paste with optimum thin film thickness without crack. The obtained sheet resistance of thin films was between 5.10 – 5.77 $\text{M}\Omega/\text{Sq}$ which was able to construct the DSSCs. This printing condition had limitation on the thin film thickness at only $6 \pm 0.25 \mu\text{m}$ and multiple printing had no effect on the increase of thin film thickness significantly. The conversion efficiency of DSSCs was 4%. Interestingly, this study confirmed the possibility of designing the thin film with various shapes, by which the efficiency conversion of solar energy showed at averaged 3%.

Field of Study: Imaging Technology

Student's Signature

Academic Year: 2019

Advisor's Signature

Co-advisor's Signature

ACKNOWLEDGEMENTS

I entered Chulalongkorn University and began the Ph.D. student. A lot of memories came across my mind at the moment when I started writing this acknowledgement. Many people shared their experience with me not only in research, but also student life.

Firstly, I would like to thank Associate Professor Dr. Aran Hansuebsai, my advisor, who lead me into all of the researches, and always support me in these three years. Without his generous help, my graduate student life should be very different. Beside my co-advisor, I also would like to thank, Associate Professor Dr.. Kazuhiro Manzaki, who gave me a lot of advises and support the material and laboratory equipment's.

Many thank Jasso Scholarship for Short-term Study 1 month to do research in Japan and Printing Foundation Financing Foundation of Thailand for financial support for traveling to do research at Gifu University Japan.

I would like to thank member of Laboratory from Gifu University japan, especially Mr. Horita Mr. Ikuta and Mr. Shinnapon who help me measuring the experimental data and providing useful information. Also, I have to thank Associate Professor Dr. Oratai Jongprateep Department of Materials Engineering, Faculty of Engineering, Kasetsart University who make a comment about the experiment.

Finally, I have to thank my parents and my friends. They are encouraged and supported me. Thank you for everything that gave me the opportunity to study in Chulalongkorn University.

Krairop Charoensopa

TABLE OF CONTENTS

	Page
ABSTRACT (THAI).....	iii
ABSTRACT (ENGLISH).....	iv
ACKNOWLEDGEMENTS	v
TABLE OF CONTENTS	vi
CHAPTER 1 INTRODUCTION	1
1.1 Significance and Background of Research Problem.....	1
1.2 Objectives of Research Project	4
1.3 Expected Benefits	4
Chapter 2 Literature Review.....	5
2.1 Titanium dioxide	8
2.2 Printing Technology	11
2.3 Solid freeform fabrication (SFF)	13
2.4 3D printer types.....	16
2.4.1 Technology of 3D Printer	17
2.4.1.1 Fused Deposition Modeling (FDM)	17
2.4.1.2 Liquid Deposition Modeling (LDM).....	19
2.5 How to make a 3D printer.....	20
2.6 Dye Sensitized Solar Cell	24
2.6.1 Basic Operating Principle	25
2.6.1.1 Excitation	25
2.6.1.2 Charge transfer	26

2.6.1.3 Dye regeneration.....	27
2.6.2 Conversion efficiency	28
2.7 Related research	29
CHAPTER 3 METHODOLOGY	33
3.1 Equipment and chemicals	33
3.1.1 Experimental equipment.....	33
3.1.2 Chemicals	35
3.2 Procedures.....	36
3.2.1 LDM 3D printer Assembly.....	36
3.2.2 Preparation of TiO ₂ paste	37
3.2.3 Rheology measurement	37
3.2.4 Printing test	37
3.2.5 Design of thin films	38
3.2.6 DSSC assembly	39
3.2.7 Thin film characteristic analysis	40
Chapter 4 Results	42
4.1 Rheology property of nano titanium dioxide paste	42
4.2 Printing test	43
4.2.1 Effect of nozzle size	43
4.2.2 Effect of printing speed, air pressure parameter and nozzle size	43
4.2.3 Effect of the distance between nozzle tip and electrode surface	46
4.3 Sheet resistance of thin film.....	48
4.4 Thin film characteristics	50
4.5 Multi-layer printing.....	50

4.6 Conversion efficiency of DSSC.....	52
Chapter 5 Conclusion and Discussion.....	54
REFERENCES	57
VITA.....	64



CHAPTER 1

INTRODUCTION

1.1 Significance and Background of Research Problem

3D printing (3D) is a technique to create three dimensional objects starting from digital models. 3D printing technology has been developed rapidly in the last few years and has shifted from traditional usage, that is, rapid prototyping. In fact, 3D printing has been used extensively in a wide range of manufacturing sectors, from aerospace, automotive to biological engineering [1].

Currently, stereo-lithography, selective laser sintering, selective laser melting and fused deposition modeling (FDM) are widely used as additive production methods and are validated both in educational institutions and in the environmental industry. Different 3D printing technologies vary in terms of cost, maximum spatial resolution, and the type of material used. The methods with 3-D features of very high spatial resolution represent the technique with high cost and the need of skilled personnel [2]. Interestingly, FDM has been recently popular among unskilled personnel with cost-effective way to produce fine 3D objects that approaches 40 μm [3]. This technique is a heat driven process that requires the melting of thermoplastics before extruding. It shows certain limitations related to the material to be deposited as small amount of polymer is easily processed with this technology (with poly (lactic acid) - PLA and acrylonitrile - butadiene - styrene - ABS is one of the group most widely used [4]. Recently, the FDM guidelines have demonstrated the high level alignment of short reinforcing fibers in composites using polymers during fiber extrusion, resulting in 3D printing components with unique structure properties. In addition, the potential of FDM technology for the invention of electronic sensors recently demonstrated the 3D printing of solid fibers obtained from the distribution of conductive carbon black to the commercial solutions of Poly (caprolactone) (PCL) DCM, followed by solvent evaporation to create a solid filament that is compressed in a 3D FDM printer[4]. Although the guidelines presented in this work help to print 3D objects with embedded sensors and electronic functions in a relatively simple

way, it requires additional steps for the production of rigid composite fibers (nano) to heat and dissolve for processing with standard 3D FDM printers.

Today, solvent-based 3D printing has become a versatile and cost-effective strategy to overcome some of the limitations set by the FDM method [5]. This new technology consists of the additive accumulation of the material layer directly from the solution in the volatile solvent. With this technology, computer control moves along the x, y and z axes, a nozzle dispensing device with a nozzle with 100 micrometers of internal diameter, beginning with the PLA concentrated solution in DCM [6]. In addition, by spraying a metallic layer for only a few tens of micrometers onto a 3D printing structure, it is able to accept conductive objects. However, in an attempt to solve this problem, 3D printing techniques have been developed in the work for printing to create a 3D microstructure of nanocomposite as a liquid conductive medium, using a syringe. This method is called Liquid Deposition Modeling (LDM) similar to the previously proposed FDM method. The advantage of LDM is the low cost system for available materials and the ability to change the assembled parts.

Solar energy is an alternative energy source that is naturally renewable. It is clean energy without pollution and with high potential. It is a source of energy that is currently popular in use. It can be converted into electrical energy by means of a device called Solar Cell. Solar energy is clean and causes no pollution to the environment. It is without movement or friction during operation and without noise, wear and tear. It requires minimal maintenance and is easy to use. It has an enormous amount and importantly is generally available especially in tropical countries like Thailand that is situated near the equator. It provides a gigantic source of energy to be acquired at no cost. In general, utilization of solar energy can be divided into two main areas, namely for generating electricity and producing heat.

Alternative energy means energy that is used instead of fuel. It can be categorized by sources into two types including exhaustible energy such as coal, natural gas, nuclear, oil shale and oil sands, etc.; and the other type is a renewable energy such as solar, wind, biomass, water and hydrogen etc., as clean energy that is innocuous to the environment. Solar energy plays an important role as an alternative

energy increasingly used in everyday life. To convert solar energy into electric energy through solar cells is very expensive [7] due to a high cost of production. It may also be disadvantageous in the production process because solar cells contain silicon which has gone through a purification process and is in a form that is ready to make solar cells but fragile in the production process.

Accordingly, Dye-Sensitized Solar Cells (DSSC) has been invented. Titanium dioxide (TiO_2) with nano-crystalline structure in DSSC has become a material used to convert solar energy into alternative electric energy as it is effective and easier to implement and is likely to be more economically cost-effective [8]. DSSC is a solar cell that does not have a PN fringe of a semiconductor but a fringe of semiconductor and liquid dye which has good properties to absorb light in the ultraviolet and visible regions depending on the type of sensitizer [9]. The principle of operation relies on the conversion of solar energy into electric energy which has a mechanism similar to the photosynthesis process of plants which does not pollute the environment. It has a simple production procedure and process [10].

This research investigated the fabrication of nano Titanium Dioxide thin film using 3 D printers instead of the traditional printing system with restrictions on controlling thickness or multiple-layer coating in one work piece. The experiment used a Liquid Deposition Modeling (LDM) 3D printer. The principle that is based on the TiO_2 paste extrusion into a shape in plane axial first and the next layers will be printed. The research examined the flow condition of the mixture of nano- TiO_2 paste with 99.5% ethanol and determine related parameters of printer such as air pressure, speed, distance between the nozzle and the electrode plate, and the nozzle size to fit the flow conditions of TiO_2 paste. The thin films were baked at 500 ° C temperature for 4 hours and then immersed in the dye for another 4 hours. An analysis was performed to determine the smoothness, thickness and electrical conductivity of the thin film nano- TiO_2 . The obtained electrode was then sandwiched with another electrode plate with electrolyte filled between the plates. The efficiency of solar cells (η) in conversion of solar energy into electric energy was measured. A comparison was made on the number of layers of titanium dioxide.

1.2 Objectives of Research Project

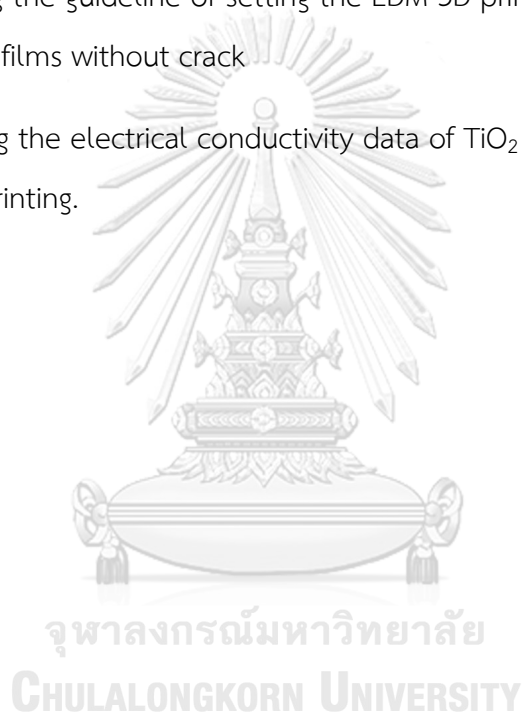
1. To study the effect of 3D printer's parameters on the quality of TiO_2 thin film on photo-electrode of DSSC.

2. To investigate the electrical conductivity of TiO_2 thin film on photo-electrodes.

1.3 Expected Benefits

1. Acquiring the guideline of setting the LDM 3D printer's parameters to fabricate TiO_2 thin films without crack

2. Obtaining the electrical conductivity data of TiO_2 thin films on photo-electrode by 3D printing.



Chapter 2

Literature Review

Energy crisis is one of the most critical concern. Insufficient petroleum and natural gas production and pollution due to usage of energy from combustion become a severe problem. We believe that the global reliance on exhaustible natural resources will be shifted to renewable energy sources in order to provide energy in an economically viable way. It is reported that nearly 30 TW (1012) of new power will be needed in 2050 [11]. One choice of renewable resource that has the capability to meet the growing energy demand comes in the form of solar radiation. The direct conversion of solar energy to electricity by photovoltaic technologies represents a rapidly growing market of electric products. Even there are a large number of options for solar absorber materials and device architectures, but Dye Sensitized Solar Cell (DSSC) is an attractive energy conversion device which produces environmental friendly energy as shown in Figure 2.1.

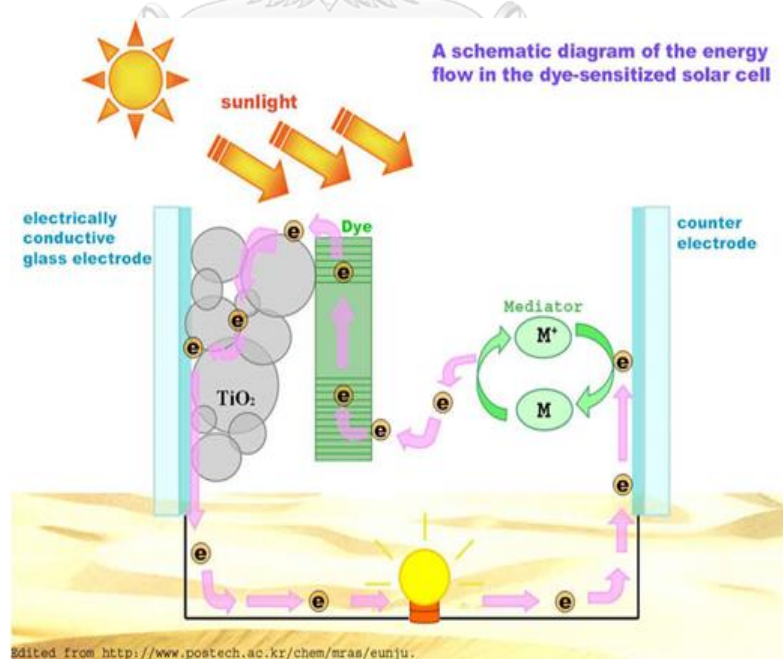


Figure 2. 1 A schematic diagram of energy flow in DSSC device

DSSC technology is based on cells made of two opposite conductive substrates: the first one (photo electrode) is coated with porous nano-crystalline TiO_2 , while the second one (counter electrode) with Pt or graphite. The electrodes can be glasses. These glasses are covered with a transparent conductive oxide (TCO) of a thickness lower than $1 \mu\text{m}$, usually a fluorinedoped tin oxide (FTO) is used.

Dye molecules are adsorbed on TiO_2 by dipping the photoanode into a dye solution. The electrons of these molecules, excited by light, are infused into the conduction band of TiO_2 and subsequently transferred to the FTO that attaches on the glass. The electrons can be recovered by a redox reaction with the electrolytic solution enclosed into the cell. The reduction of the electrolyte occurs at the counter electrode catalyzed by the Pt.

DSSCs can be designed in several types. The most popular one is composed of three parts: a dye-sensitized nanocrystalline thin film photoanode, a redox couple (usually I^3^-/I^-) in organic solvent(s), and a platinized transparent conducting oxide glass as a counter electrode. It should be noted that the iodine-iodide redox electrolytes may have some disadvantages such as its oxidizing nature especially in the presence of moisture, photocurrent loss due to visible light absorption and significant loss in short circuit current density particularly in highly viscous electrolytes [12]. Thus, another type of DSSC is proposed as solid-state dye-sensitized solar cells.

Interestingly, the characteristics of thin film electrodes will pave a new way to develop more efficient of all types of DSSCs opening up a new perspective for industry. Several materials can be used as a thin film such as TiO_2 , SiO_2 and so on. Among those materials, TiO_2 is an attractive material to apply for most DSSCs as it does not only have high refractive index but also being hydrophilic property [13].

This research was based on the fluid iodine-iodide redox systems, penetrated inside the porous TiO_2 thin film and facilitate charge transport and diffusivity of

charges, giving rise to such an acceptable cell performance. To consider the fabricating techniques, broad ranges of method have been developed with different capabilities as their fundamentals are diverse. Screen printing, inkjet printing and solid freeform fabrication (SFF) technologies such as stereo-lithography, selective laser sintering, selective laser melting and fused deposition modeling (FDM) are among the most widely used in thin film fabrication as they possibly control film thickness and its porosity [14, 15]. SFF methods are based on the principle of three-dimensional (3D) printing.

The existence of these technologies differ in terms of cost, maximum spatial resolution and type of materials used. For example, the FDM technology was recently demonstrated to fabricate the electronic sensors [16]. However it still requires the additional step of the production of a solid (nano) composite filament to be heated and melted in order to be processed with a standard FDM 3D printer.

Liquid deposition modelling has emerged as an alternative and cost-effective technique to overcome some of the limits imposed by the FDM approach [17]. The concept is the additive deposition of material layers directly from a solution or paste in a volatile solvent. By means of this technology, the production of freeform structures was achieved by using an extruding nozzle and a computer-controlled robot moving along the x, y and z axes. A low-cost commercial benchtop 3D printer equipped with a syringe dispenser could be employed.

The rheological behavior of dispersed micro or nano-particles is important at varying solid content and its printability is identified based on the shear-rate of the material at the extrusion nozzle without heat. It is noted that we may call this methodology in another term as “low temperature deposition manufacturing” (LDM) as there is no need to produce a solid filament like FDM technique. Using a uniform homogeneous dispersion of liquid/paste is a key factor of 3D printing. It is because of the high tendency of particles to form bundles and aggregates that may cause clogging of the nozzle and flux instability during the printing process. In addition,

printing speed and shear-rate of the dispersion at the extrusion nozzle needs to be controlled. Therefore, an appropriate material concentration is required to obtain a thin film without the fracture of surface [18].

Our research studied the use of a commercial nano- TiO_2 paste for fabricating a thin film on a photo electrode by using LDM 3D printing method. The printers' parameters such as nozzle size, printing speed, air pressure and the distance between the nozzle tip and an electrode's surface were investigated to optimize the set-up of the printer. The thin film characteristics such as thickness, uniformity, crack-free, resistivity and photovoltaic efficiency were observed. This research will be of useful for scientists who are engaged with DSSCs.

2.1 Titanium dioxide

Titanium dioxide (TiO_2) is an important material due to its potential application in electronic devices such as conductive thin films for solar cells, memory devices and sensor applications [19, 20]. Non-toxicity, environmental compatibility and low price are advantages of TiO_2 . In addition, chemical stability, transparency in the visible region, high dielectric constant and high refractive index of TiO_2 thin films give more attention to the electronic industry. TiO_2 has three different crystal phases: Anatase (tetragonal), Rutile (tetragonal) and Brookite (orthorhombic) as shown in Figure 2.2. As the electrical properties of thin films are related with crystals structure, TiO_2 phases thus are essential to predict the material behavior and their potential application in electronic devices. Among all phases, Anatase has the best photocatalytic activity resulting in the highest photocatalytic efficiency. Rutile has the highest density and refractive index among the three phases; it is primarily used for functional coatings in optics, photonics and microelectronics industries. While Brookite has been rarely used, mainly due to its complex synthesis as a pure phase [21, 22].

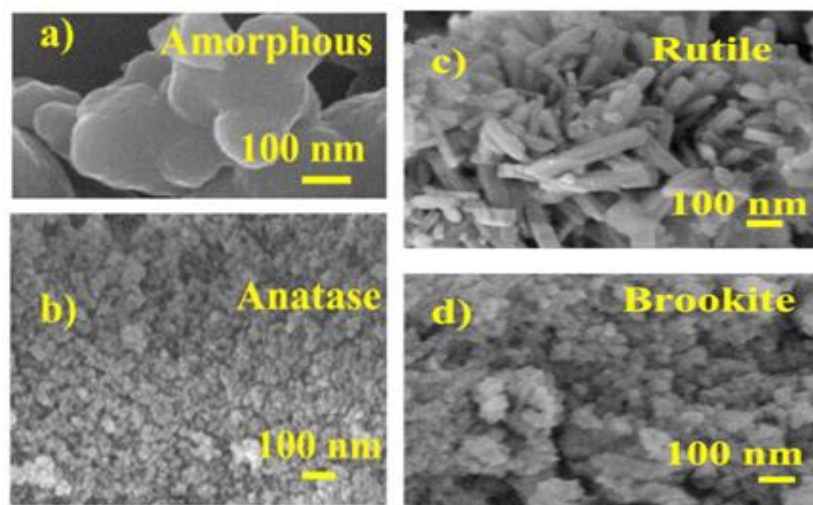


Figure 2. 2 SEM micrographs representing: a) amorphous titania; b) anatase; c) rutile and d) brookite [21]

Although TiO_2 has its high resistivity, but compensation is possible as these thin films have a high energy gap [23, 24], whereby impurity band conduction may become significant even above room temperature. Thus, electrical conductivity processes are mainly due to hopping via impurity centers. Anatase TiO_2 electrodes are mostly used in solar cells, lithium batteries and electrochromic devices[25] . While TiO_2 -based nanotubes have attracted wide attention owing to their potential for application in highly efficient photocatalysis [26].

To fabricate TiO_2 thin films, although chemical vapour deposition, sputtering and sol-gel methods were reported [27], but also printing techniques such as screen printing and inkjet printing were also employed [28-32]. For these printing processes, the properties of ink such as particle size, rheology, jetting performance, wetting and adhesion on substrates, should be optimized in order to achieve uniform deposition. Post-printing step such as sintering is also important factor in TiO_2 fabrication. It should be noted that the appearance of cracks occurred when the critical value of thin film thickness is reached, but withdrawal speed has to be controlled to prevent the thickness of the films producing cracks and bubbles after sintering. There are some features of crack to appear: rosette which can be observed over the whole

surface at lower viscosities while a long straight lines obtained from the solution with higher viscosity.

To consider ink rheology for printing, the effect of solvent content in the TiO₂ paste is crucial for printed and sintered TiO₂ thin films. The correlation among paste rheology, layer properties and the DSSCs efficiency depending on the solvent content was studied [33]. The results confirm the importance of controlled solvent concentration and rheological properties of TiO₂ pastes for higher DSSC efficiency achievement.

Nowadays there are TiO₂ paste finished products available in the market for thin film printing. Three kinds of commercial TiO₂ powders are provided: P25 (av. 30 nm - 80% anatase and 20% rutile); ST21 (av. 25 nm - 100% anatase) and ST41 (av. 160 nm - 100% anatase)[34]. The powders are mixed with vehicle (resin + solvents such as ethyl celluloses in toluene/ethanol) and then are grinded with a three-roller-mill. To adjust flow-ability and some properties, solvents and other additives will be added. Note that both water and alcohol may induce TiO₂ aggregation and yielding poorly reproducible results. Thus, α -terpineol-based pastes is a choice as they are stable at long-term and give reproducible results for several year. However, it is noted that to make a good linkage among TiO₂ particles and between a TiO₂ particle and a conductive oxide surface of substrate, hydroxides (-OH) have to be on the surface and make strong chemical bonding between each other by dehydration at sintering. The aggregates in matrix should not be occurred. This can create the cracks and shrinkage of the film, resulting in the peering-off from the substrate. Accordingly, the proper combination of solvents in the paste is important for keeping the porous- TiO₂ layers mechanically stable during sintering to protect the cracks and peeling-up from substrate.



where, M_1 denotes a titanium atom of a particle and M_2 denotes a titanium atom of another particle or an atom on a conductive oxide substrate.

To consider the thin film layer, It has been reported that particles over 100 nm can diffuse visible light effectively [35] Hence, ST41 (av. 160 nm) was able to diffuse visible light. This is the reason why the layer of ST41 was white and opaque. In addition, a high-performance DSSC requires large surface area TiO_2 electrodes with high porosity so that dyes can be sufficiently adsorbed and electrons can be quickly transferred.

2.2 Printing Technology

Nowadays printing technology has been developed for standards in press and post-press stages. Thus, thin film fabrication such as TiO_2 , Pt and Ag on conductive substrates does not need additional development but a simple controlling of ink/paste characteristics. The parameters involved in the printing processes can be optimized by analyzing the paste rheology through the Newton law for ideal liquids.

Inkjet printing has been found to be a very promising and useful method for material deposition, and even semiconductor films can be deposited directly from a colloidal dispersion (ink) onto a large variety of substrates. The features of inkjet printing is one-step processing, inexpensive and compact equipment, and applicability to a various substrates. By this technique, liquid (in droplet form) often turns into solid via cooling, chemical changes or evaporation. Continuous Inkjet printer uses fluids with lower viscosity at higher drop velocity than Drop-On-Demand (DOD) system and is mostly used where printing speed is important. In contrast, DOD is used where smaller drop size and higher accuracy are required, and it has fewer limitations on ink properties as compared with Continuous system.

The physical properties of ink are an important aspects of inkjet printing. Viscosity, surface tension and inertia are the three factors which affect the behaviour of droplets and liquid jets. The viscosity of ink should be adequately low since the power produced by the piezoelectric diaphragm is limited. On the other hand,

surface tension should be sufficiently high to avoid ink dripping from the nozzle. The surface tension and viscosity (usually below 0.025 N/m and 1–20cP, respectively) are reported to give proper droplet formation and correct spreading over the substrate upon contact [36].

Earlier research used the TiO₂ ink with the average particle size at around 25, 32 and 28 nm for anatase, rutile and brookite, whereby the obtained printed films were uniform, with thicknesses of 70, 140 and 130 nm for anatase, rutile and brookite respectively [36]. Cherrington et al. reported the formulation of suitable inks of TiO₂ nanoparticles for inkjet printing for dye solar cells [37]. Melis- Arin et al. demonstrated the printed TiO₂ thin film using inkjet printing of aqueous suspensions containing TiO₂ nanoparticles which was satisfied with cost-efficient for mass production [38].

Regarding inkjet ink, agglomeration of TiO₂ nanoparticles can occur in the colloids. This leads to the dispersions possibly dominated by secondary particles in the micron range. This is a drawback of inkjet printing, since the presence of large agglomerates could result in the blockage of the nozzle of printers. Therefore, the use of a dispersing agents is necessary to increase the electrostatic repulsive force, which deducts agglomeration, and subsequently reduces the particle size of the dispersion.

Screen printing is another method used for conductive thin film fabrication. This method is low cost and able to control the thickness of TiO₂ films with high porosity. Several researches employed this technique to fabricate the TiO₂ thin films [30–32]. The obtained thin films could achieve over 17 μm thickness for an anode electrodes of DSSC [34]. A conversion efficiency of 8.7% was obtained at a single-layer of TiO₂ thin film. While 9.2% was obtained at double-layers composed of transparent and light-scattering TiO₂ films.

The principal of screen printing is based on a screen made of a synthetic fibre or steel mesh. On the screen, an image is designed to transfer ink/paste onto the substrate by squeegee pressure through the mesh. Today, it is possible to adjust the thin film's thickness with extreme precision (± 500 nm) by this method [34]. We must control printing speed, the pressure and angle of the squeegee, the number of squeegee runs, the distance between the screen and the substrate and its velocity. In addition, the screen's parameters need to be considered such as screen type, mesh count, mesh opening, thread diameter, opening area and thread thickness. However, it is reported that screen printing technique tends to be suitable for large-area DSSC: prototype modules of 30×30 cm² [39, 40].

Ink/paste viscosity should be high enough to avoid percolation under the mesh and to permit a correct deposition forming (thixotropy). Thus it is necessary to control the rheology property of ink/pastes to optimize the quality of thin film. TiO₂ paste can be cured by UV or IR radiation.

For rotary screen printing or roll-to-roll processes, the transfer occurs by contact between the cylinder and the substrate: the squeegee presses on the substrate in the contact point and transfers the pattern through the meshes of the screen. This technique is aimed for largescale mass production and is faster than other printing techniques, but the resolution is limited.

2.3 Solid freeform fabrication (SFF) UNIVERSITY

SFF is a method to fabricate objects by controlling the placement and adhesion of successive layers of a material in 3D space. This technique is also known as 3D printing or “additive layer manufacturing” (ALM) [41, 42]. To print an object, a digital model is created using a computer aided design (CAD) application, or some other variety of 3D modelling software. Alternatively, the digital model may be captured by scanning a real object with a 3D scanner, or derived from a 3D scan that is later manipulated with CAD or other software tools.

The SFF techniques are classified into three main groups as shown in Figure 2.3. The first group is laser based systems such as Stereolithography (SL) and

Selective laser sintering (SLS) processes. The others are droplet-based and nozzle-based respectively. Much attention has been paid to nozzle based system, particularly extrusion-principle in recent years as it is mechanically simple process using pressure-assisted syringe and a wide range of materials can be processed effectively.

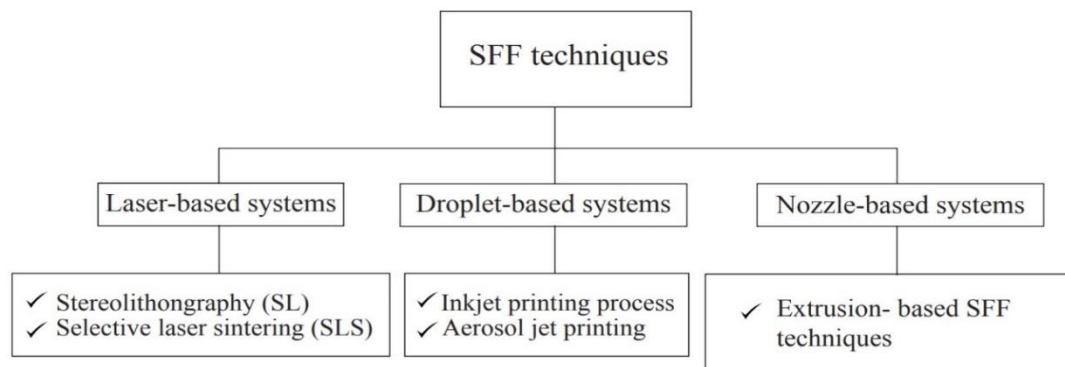


Figure 2. 3 Classification of different SFF techniques for fabrication thin films

The paste is fed into an extruder that is connected to a pump and the fabrication process is accomplished in heat environment as fused deposition modelling (FDM) [43, 44]. This system has been recognized to be advantageous for fabrication of different kinds of nano-materials. In addition, researchers have made attempts to develop new configurations to process the materials without melting that can preserve the property of the original materials. Pressure-assisted micro-syringe (PAM) and low-temperature deposition manufacturing were proposed [45, 46], whereby a new three-dimensional (3D) printing system was developed. The layer of deposited materials is laid-down on the platform. After forming the wet film, baking is needed to remove the solvent. Fig.2.4 illustrates the principle of the extrusion-based methods schematically.

Note that the choice of viscous paste or other fluid materials is a big topic of research in additive manufacturing world. Plastics are easier to form multilayer as they will set at room temperature; while wet or paste materials such as TiO_2 or clays, there are some limitations due to geometries, collapses, drying and shrinkage. Thus

the material extruded becomes a key role for obtaining acceptable final results. The adjustment of printer's parameters can affect the uniformity, thickness and quality of printed thin films. These parameters are nozzle size, printing speed, pressure and distance of the nozzle tip from platform, as they relate to the quality of printed thin film such as thickness, uniformity and crack.

To achieve uniform structure, nozzle size should be selected appropriately according to particle size/shape and flow ability of the paste. Generally, if the nozzle size is too small the paste is dispensed sporadically, and if the nozzle is too big the paste may be over-run.

Printing Speed (Speed while Extruding controls the printing head moving while extruding the paste. Low printing speed may be preferred to achieve good quality of printed film. Increasing the printing speed can get some prints a bit faster than usual, however too much increase of the speed may result in failing to construct the print uniformity as dispersion of TiO_2 particles in paste is disturbed. Crack will be occurred.

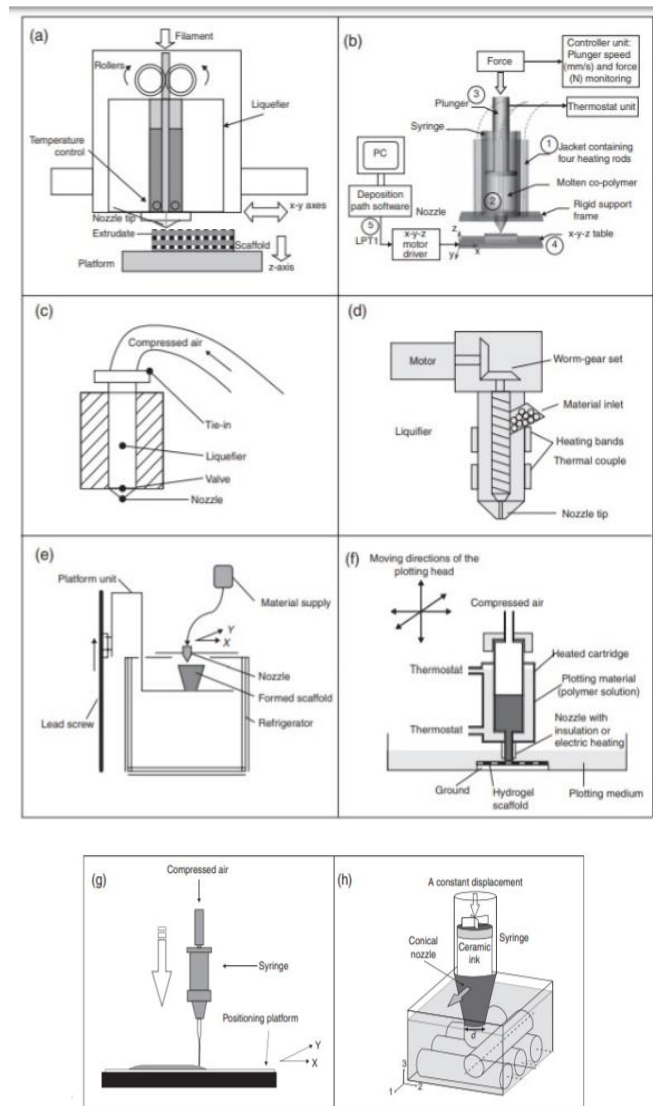


Figure 2. 4 Schematic of extrusion-based equipment

2.4 3D printer types

“3D printing” is a common name under the SFF technique. Some industries refer 3D printing system as Additive Layer Manufacturing (ALM), but we’ll use its practical name here—3D Printing. There are different types of 3D printers depending on cost, print quality, maximum speed, capability, practicality and user expectations.

The technologies and materials used are varied, including the way of ink/paste extrusion to substrates. The machines are no longer difficult for home users such as the users can create a virtual design (3D model) of the object they want to print in 3D; and they can save their design as a Computer Aided Design file, or CAD.

The advantages of this printing system are able to vary the numbers of printed layer as well as different levelling pattern of thin films by one time operation.

Liquid Deposition Modeling (LDM) printer was in our interest as its extruder could be used for thin film fabrication by using wet or paste materials like clay, alumina and TiO₂.

The LDM 3D printer is based on a pneumatic system in which a pump pushes the paste through the extruder. With this technology it is possible to accurately control the flow of material and also use retraction to interrupt deposition. Another version of design is syringe extruder. It is an alternative for other applications.

2.4.1 Technology of 3D Printer

To Identify the 3D printer most suitable technologies for this research, it is classified into two printing technologies described below. In addition to the Process, Materials and Application Areas, the Strengths and Weaknesses are also described for each one of them.

2.4.1.1 Fused Deposition Modeling (FDM)

(a) Process, Materials, Application Areas

This type of printer typically works with plastic filament. The technology behind this is often referred to Fused Deposition Modeling (FDM) as shown in Figure 2.5. The process is done by extruding a thermoplastic polymer through a heated nozzle which gets deposited on a bed. FDM is also considered to be a form of additive manufacturing, which at the same time is a “process of joining materials to make objects from 3D model data, usually layer upon layer. Creating a 3D printed object through FDM requires, in the first place, to work on a STL file (stereo lithography file format) which mathematically slices and orients the model for the next building process. Sometimes, the software is capable of generating support structures for the object automatically. The process involves a plastic filament which is fed by a spool to the nozzle where the material is liquefied and “drawn” on the

platform. The filament hardens while being gradually deposited, following a certain structure, in order to create the final 3D print. When a layer is drawn, the platform lowers by one layer thickness so that the printer is able to start working on the next layer. There are many different materials which can be used with FDM. In the first place, they are divided between the industrial and the consumer categories. The most commonly used are ABS (Acrylonitrile Butadiene Styrene), PLA (Polylactic Acid) and Nylon (Polyamide), but other exotic varieties of materials can also be used, like blended and functional materials. It is because this technology presents some very good pros, FDM is often used in the area of both nonfunctional and functional applications.

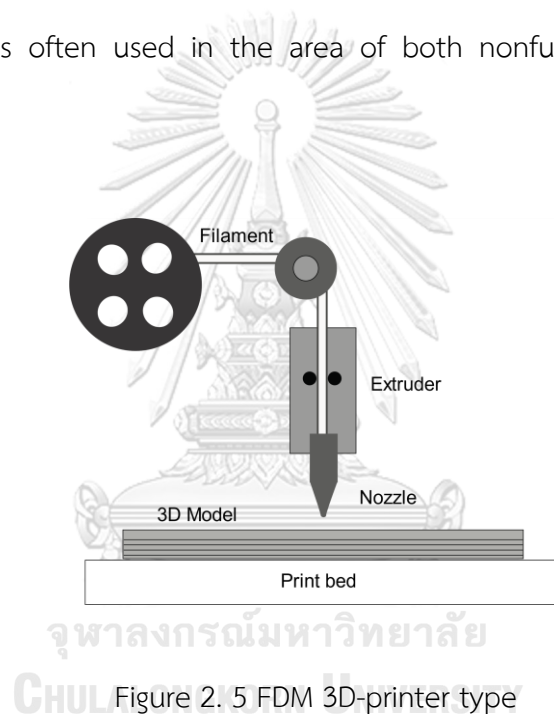


Figure 2. 5 FDM 3D-printer type

(b) Strengths and Weaknesses

FDM printers are among the cheapest and most affordable especially for those who want to use it in a domestic environment. In addition, it is considered to be a very clean technology, usually simple-use and office-friendly. The technology can also produce complex geometries and cavities that would otherwise be quite problematic.

The precision of the machine is dependent on the extruder movements on the x and y axis, but there are other factors to be taken into consideration. For example, the bonding force between the layers is lower than in the Stereolithography process. Consequently, the weight of the layers might squeeze the lower layers, which can therefore influence and even compromise the quality of the 3D print. Contrary to SLA, FDM presents also an increased complexity. One needs to keep in mind weight and size, but also constraints. It is very important to make sure that a print can meet the expectations that one sees on the screen when first modelling. The constraints in this case depend on several factors, but mainly on the material chosen, through which it is possible to understand how big an item can be printed through FDM.

2.4.1.2 Liquid Deposition Modeling (LDM)

(a) Process, Materials, Application

Liquid Deposition Modeling (LDM) was developed by the WASP Company, using its extruder for ceramic materials as shown Figure 2.6, which can be adapted to most 3D printers on the market today. The manufacturer focuses on the development of systems that allow the use of functional or end-use materials like ceramics, porcelain, clay, alumina, zirconium and other advanced ceramics, in order to promote digital handicraft and self-production. The LDM Wasp Extruder is based on a pneumatic system in which a pump sends the paste ceramic materials through to the deposition arm. With this technology it is possible to accurately control the flow of material and also use retraction to interrupt deposition. Innovations also include a system which eliminates air bubbles in the mixture and an outward pressure multiplier up to 40 bar in the screw extruder.



Figure 2. 6 LDM 3D printer type by WASP

(b) Strengths and Weaknesses

Advantages	Disadvantages
Low cost of systems	Limited part geometry
Limited layer resolution	Very Large size part capabilities
Wide range of materials available	Difficult to operate properly

2.5 How to make a 3D printer

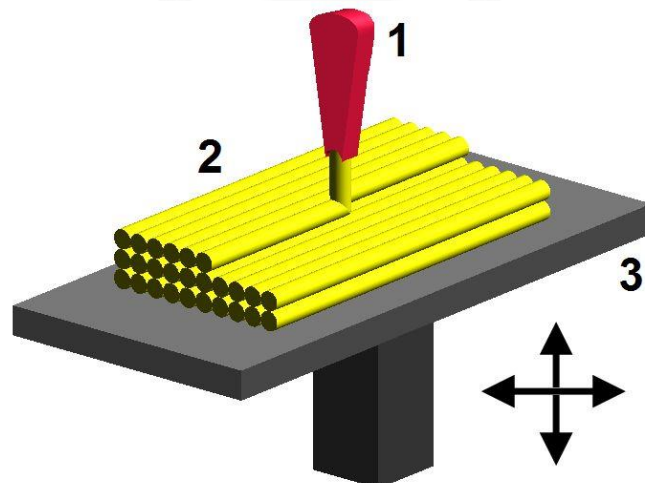


Figure 2. 7 Moving direction of a nozzle in 3 ways

The mechanism of a 3D printer is to extrude little drops/line of molten plastic or paste from a headed tip (nozzle) on a substrate with the surrounding air, in cools

down into a solid state. The printer moves its nozzle in 3 ways to deposit the materials in a 3D model as shown in Figure 2.7. The smaller the drops/lines it deposits, the smoother the print would be.

To make the simple FDM or LDM printers, we can do by ourselves. The necessary parts need to be purchased as followings:

- Heat bed
- Extruder
- Stepper motor
- 12 Volt 10 Amp Power Supply
- 5 x 8 Shaft Coupler
- Trapezoidal Threaded Screw
- 8 x 22 x 7 mm Radial Bearing
- Limit Switch
- Acrylic Sheet
- Wooden/ metal frame
- circuit parts
- pump etc.

จุฬาลงกรณ์มหาวิทยาลัย

The circuit parts include main board and driver as shown in Figure 2.8. An extruder is used for pushing the plastic filament or paste inside the nozzle. For FDM type, the plastic filament must be melted, and this melted plastic goes inside the hot nozzle. It will solidify on the hotbed. This part consist of Cooling Fan, Nozzle, Heater, Temperature Sensor and Teflon Tubing.

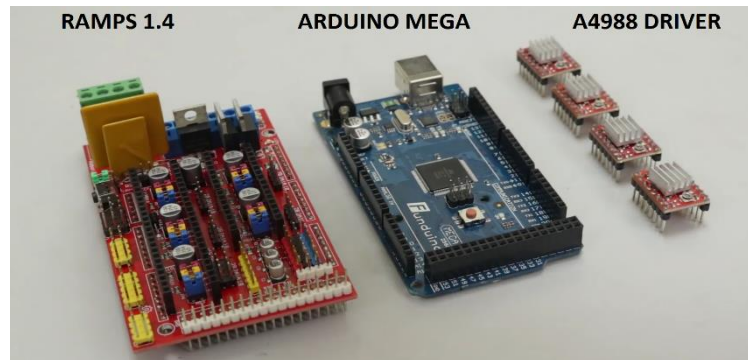


Figure 2. 8 Board and driver of printers

12V and 10A Power supply is important. Thick gauge wire is recommended for output. It is because heater consumes lots of power so high current flow through this wire. .

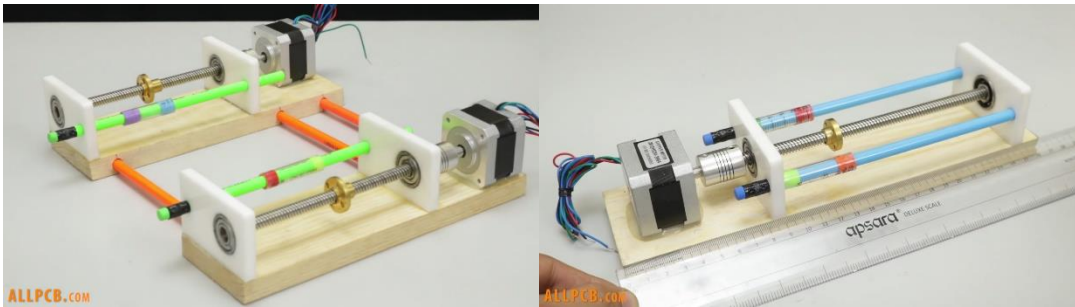


Figure 2. 9 power supply 12V 10A

3D Printer is working on 3 axis, x, y and z. To make a y-axis arrangement, 2-stepper motor is needed. For x- and z-axis arrangement, it should relate to y-axis arrangement as shown in Figure 2.10. 3D Printing is done on a bed. Keep in mind that the bed must be at the proper leveling. If it is not in level, the printed object will not be accurate. Figure 2.11 shows the bed arrangement. Then the x- and z-axis will be joined with the y-axis over the bed. Two wooden blocks on the x-axis shall be attached as shown in Figure 2.12..

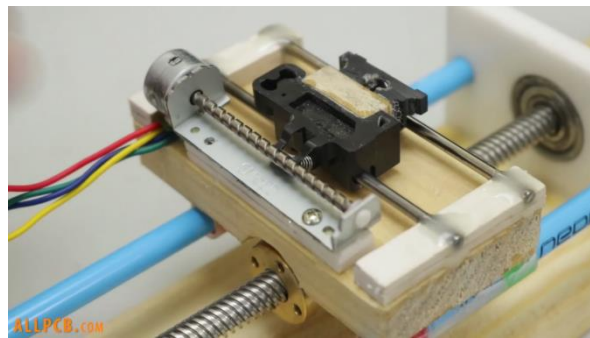
- x-Axis: It controls the movement of the nozzle to left and right
- y-Axis: it control the movement of bed

- z-Axis: It controls the movement of the nozzle up and down.



y-axis

x-axis



z-axis

Figure 2. 10 The arrangement of x-,y- and z-axis

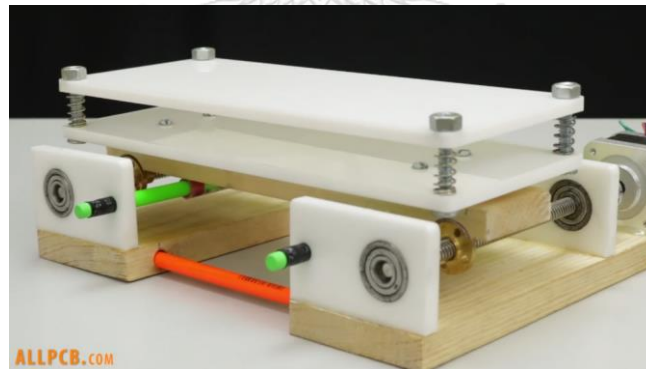


Figure 2. 11 Bed arrangement

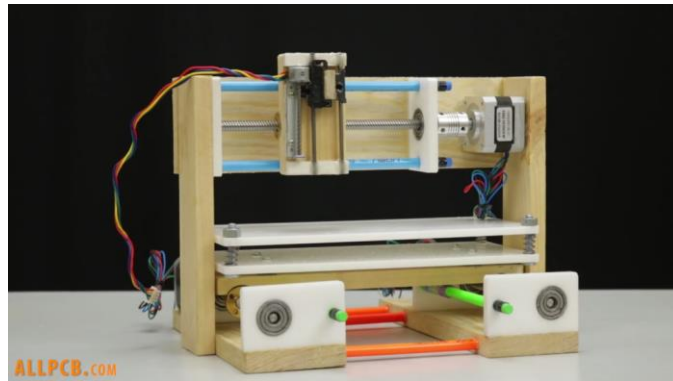


Figure 2. 12 x-,y- and z-axis moving parts on bed

An extruder will be fixed in the right position. Finally, we can install the assembly parts in a frame.

2.6 Dye Sensitized Solar Cell

The first attempt to generate electricity from DSSC was from ZnO sensitized with Chlorophyll [47]. It was sometimes referred to as 'Artificial Photosynthesis'. The first embodiment of modern day Dye-sensitized Solar Cell (DSSC) dates back to late 1980 [48]. However, not until the fundamental work of Grätzel and O'Regan in 1991 [49], it was proven that DSSC can be a feasible alternative energy source. The reported conversion efficiency for DSSC with conventional Ru-based dyes was around 11.5% [50, 51]. Recently, a Zn-based dye and Co-based electrolyte pair have been developed and their conversion efficiency has exceeded 12% [52]. Although the power conversion efficiency of DSSC is not as good as those compared to other inorganic solar cells, but it is temperature-independent under normal operating temperature range of 25–65 °C. While the conversion efficiency of Si solar cells declines by 20%.

A key requirement for all types of solar cells is long-term stability. From different extensive studies, it has been confirmed that the DSSCs can satisfy the stability requirements for commercial solar cells to endure outdoor operation for 20 plus years. Considering this advantage, DSSC has the potential to be a feasible candidate for the race of large-scale solar energy conversion systems.

2.6.1 Basic Operating Principle

The DSSC uses the same basic principle as plant photosynthesis to generate electricity from sunlight. Each plant leaf is a photo-chemical cell that converts solar energy into biological material. Although only 0.02-0.05% of the incident solar energy is converted by the photosynthesis process, the food being produced is 100 times more than what is needed for mankind [53]. The chlorophyll in green leaves generate electrons using the photon energy, which triggers the subsequent reactions to complete the photosynthesis process.

The DSSC is the photovoltaic device that utilizes separate mediums for light absorption/carrier generation (dye) and carrier transport (TiO_2 nano-particles). The operation steps are the following.

2.6.1.1 Excitation

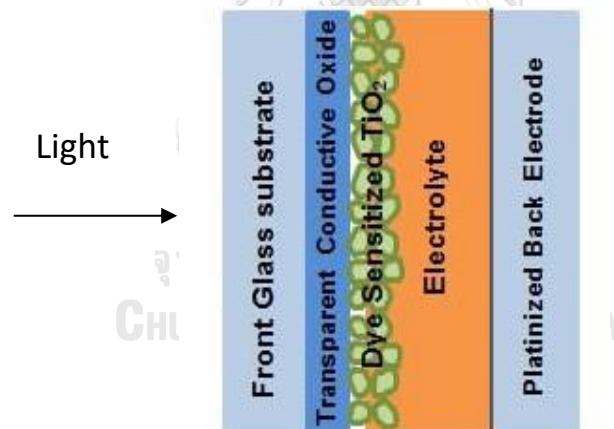


Figure 2. 13 Basic device structure and relative band diagram for DSSC.

Figure 2.13 shows the basic device structure and relative band diagram for DSSC.. The sensitizing dye molecules are adsorbed on the surface of a wide band gap semiconductor (typically TiO_2). Upon absorption of a photon (excitation), the dye gains the ability to transfer an electron to the conduction band of the semiconductor. When this happens, a hole is left behind. A mediator (M) for example iodide in the liquid electrolyte fills the hole with one of its own electrons.

2.6.1.2 Charge transfer

The nano-crystalline semiconductor anode is not only where the sensitizers adhere, but also where the charge transfer occurs. Consequently, it is acknowledgeable that the quality of the semiconductor electrode directly affects the efficiency of DSSC. Reducing charge recombination is the most direct means to improve DSSC efficiency, and the quality of TiO₂ thin film is one of the most important key. There are four fundamental requirements of the electrode material: large surface area and roughness, sponge-like nano-crystalline structure with good electronic contact. The anode material structure should allow electrolyte redox couple regenerates the oxide dye and charge should also be able to rapidly inject into the semiconductor. At the meantime, backward charge recombination should be the slowest step.

TiO₂ is an ideal material with appropriate band gap and electronic properties as mentioned. It has additional advantages like non-toxic, stable in water and better anti-corrosion property comparing to narrow band gap semiconductor material like silicon. TiO₂ has three kinds of crystal structure: anatase, rutile and brookite. Brookite only exists in natural ores and it cannot be synthesize in industry. Anatase has a band gap of 3 eV and rutile has a band gap of 3.2 eV. The conduction band density of anatase in Ti 3d is higher than that of rutile, which makes it easier to accept electrons from the top of valence band (O 2p). That is the reason that anatase TiO₂ has better performance comparing to rutile [54, 55]. These mechanics will determine the efficiency of the DSSC. TiO₂ electrode is one of the most important key to increase the efficiency because it is where sensitizers load and the electrons transfer happen. The requirements of the TiO₂ film is relate to these mentioned concepts. The purpose of this study is to manufacture a thick film printable TiO₂ paste which is appropriate for mass production and able to lower the DSSC cost.

The nonporous TiO₂ thin film consists of spherical anatase particles of diameter ~20 nm. As the TiO₂ particle diameter is too small for electric field to build up, the dominant electron transport mechanism is diffusion via trapping and de-trapping.

The electron travels through the outer circuit performing work to reach the back of counter electrode (cathode), and reduces the iodine in the electrolyte. The platinum layer on the electrode acts as a catalyst for the reduction. The dark cathode reaction:



The iodine reduction can also occur at the excited dye molecules causing recombination of the photo-generated electrons. For efficient charge transfer, the rate of iodine reduction at the counter electrode has to be orders of magnitude faster than the recombination at the TiO₂/electrolyte interface.

2.6.1.3 Dye regeneration

The reduced iodide ion replenishes the highest occupied molecular orbital (HOMO) of the dye - regenerating its original form, and makes it ready for electron generation again.

The photo-anode reaction:



This prevents the buildup of S₂, which could lead to the conduction band electrons going back to the dye molecules. The maximum output voltage equals to the difference between the Fermi level of the semiconductor and the redox potential of the mediator [56]

Thus, the device is can produce electricity from light without undergoing any permanent

physical and chemical change.

2.6.2 Conversion efficiency

We used TiO_2 as an active material that absorbs photons and converts them into electric current. This material has a band gap around 3.2–3.8 eV, allowing the effective absorption of ultraviolet light. Only a few electron–hole pairs are produced when the material is illuminated by the solar spectrum. Conversion efficiency of a DSSC therefore is the percentage of the solar energy shining on a device that is converted into usable electricity. To improve the DSSCs, light absorption properties of organic dye must be tuned to have a maximum response throughout visible and near infra-red spectrum.

To calculate the efficiency of the DSSC, we propose: $\text{Efficiency} = P_{out} / P_{in}$. To calculate P_{in} (the input power) use the area of the cell. We can measure the module area with a ruler [57] The latter dependent upon the incident light flux (I_0), and the former, implicit properties of the device itself (equation 2.3); namely the short-circuit current (I_{SC}), open-circuit voltage (V_{OC}) and fill-factor (FF). The short-circuit current density (J_{SC}) is typically reported to allow comparison between devices whose dimensions may vary ($J_{SC} = I_{SC}/\text{Area}$).

The FF is determined by the ratio ‘maximum obtainable power/theoretical obtainable power’ where the theoretical obtainable power is the product $I_{SC} \cdot V_{OC}$ (I_{SC} and V_{OC} being zero at open-circuit and short-circuit conditions respectively with Grade A solar-cells typically having $FF \geq 0.7$).

$$\text{Conversion efficiency} = \eta = (P_{out} / P_{in}) \times 100 = \frac{J_{SC} V_{OC} (FF)}{I_0} \times 100 \dots (2.3)$$

Dye-sensitized solar cells (DSSCs) have many advantages over their silicon-based counterparts. They offer transparency, low cost, and high power conversion efficiencies under cloudy and artificial light conditions.

2.7 Related research

Yuli Lin, Cheng-Yi Hsu and Chang-Lun Tai [58] studied Inkjet printing for dye-sensitized solar cells. They prepared the TiO_2 thin film electrode for dye-sensitized solar cells (DSSC) on ITO-PET substrate using a general jet-printer. The results were compared with that obtained using ITO glass substrate. In this study, the dispersion of TiO_2 slurry was manipulated by changing the pH value of the solution to avoid agglomeration of TiO_2 particles. The average TiO_2 particles used in this study were measured about 130nm. The experimental results showed that it had the best performance when the thickness of the TiO_2 thin film was about $10\mu\text{m}$. In ITO glass substrate, the measured short circuit current was about 5.03mA, the open circuit voltage was measured to be 0.65V. In ITO-PET substrate, the measured short circuit current was about 2.73mA, the open circuit voltage was measured to be 0.68V.

YU Zhaohui, WANG Huanmei and CHEN Guangxue [59] studied the effects of nozzle distance on micro quality in 3D printing. The quality of forming model was influenced by the nozzle distance. UV inkjet printer was used to complete 3D printing; the micro quality of printings under different nozzle distances were studied, and the influences of line attributes and surface attributes in micro quality caused by different nozzle distances were analyzed and discussed, in order to get the best micro quality through the nozzle distance setting. The results showed that the nozzle distance within a certain range, the influence on line attributes was greater than the influence on surface attributes caused by nozzle distance; when the nozzle distance is between 1.5-2.5mm, the micro quality of printed image is best.

Chanu Photiphitak and Sukunya Khunchan [60] studied the Improvement of the efficiency of Dye Sensitized Solar Cells by TiO_2 Blocking Layer. This research aims to improve the efficiency of dye-sensitized solar cell (DSSC) with the synthesis of TiO_2 sol gel which is modified from surfactant-assisted sol gel techniques to prepare the TiO_2 blocking layer by Dip and Spin coating methods. TiO_2 blocking layer film characterization was analyzed by SEM, XRD and UV-vis spectroscopy techniques. The

performance and internal resistance of the DSSC were studied by IV Tester and Electrochemical impedance spectroscopy, respectively. The recombination process was measured by using a transient voltage graph. The results showed that coating of TiO_2 blocking layer film by Dip coating, which has 280 nm of thickness, had a maximum efficiency at 3.75% (14.33% increase) when compared to a standard cell at 3.28%. The TiO_2 blocking layer reduces the recombination reaction at the FTO/electrolyte interface.

Syed Ghufran Hashmi et al. [61] prepared DSSCs with inkjet-printed dyes. They reported a versatile dye sensitization process, achieved by inkjet printing over the TiO_2 thin film, which produces solar cells. In addition to allowing precise control of dye loading required, inkjet printing also made it possible to freely adjust the amount and position of the dye to create DSSCs with tailored transparency, color density gradients, and patterns of one or more dyes on the same electrode. The method was confirmed to be applicable also for non-transparent, high-efficiency DSSC designs that employ a light scattering layer.

Seigo Ito et al. [34] studied the fabrication of TiO_2 thin films for dye-sensitized solar cells by screen printing. They proposed the preparation technique of TiO_2 pastes from commercially-available powders to fabricate the thin films without cracking and peeling-off over 17 μm thickness. A conversion efficiency of 8.7% was obtained by using a single-layer of a semi-transparent- TiO_2 film. A conversion efficiency of 9.2% was obtained by using double-layers composed of transparent and light-scattering TiO_2 films for a photon-trapping system.

CHENG-LUN YU [62] proposed the development of a thick film screen printable paste for the DSSC TiO_2 anode as the thick film was appropriate for lowering the manufacturing cost of DSSC via mass production. An ideal TiO_2 electrode has to achieve moderate thickness, good light transmittance, high degree of roughness and good electrical connection between the dyes and the TiO_2 layer.

TiO₂ thick film printing pastes were prepared and their properties were evaluated. Experimental methods and experimental protocols for the characterization of the TiO₂ thick film printable paste were established which could be useful in the advancement of the manufacturing of DSSC.

Md Imran Khan [63] studied the optimization of TiO₂ structure and ambient process conditions for the fabrication of thin films. TiO₂ types and morphology were found to have a direct impact on the conversion efficiency. Scanning Electron Microscopy (SEM) was used to investigate the TiO₂ nanostructure. Different chemical treatments and electrolytes were also explored towards optimizing the cell performance. Standard solar cell characterization techniques such as current-voltage and spectral response measurements were employed to evaluate the cell performance.

Supaphorn Srising [64] studied the fabrication of DSSC using natural dyes extracted from a stem bark. The electrical properties including its efficiency were studied. The natural dye was extracted from stem bark of Terminalia. It was found that the conversion efficiency of DSSC depended on the dye concentration. Although it was relatively low compared with the standard Ruthenium complex dye (N719 dye), this might be due to the unstable of natural dyes.

Buppachat Toboonsung [65] studied the effect of annealing temperature on electrical sheet resistance. The experiment was carried out by titanium wires as electrodes of the sparking process and varied the sparking time 1-4 h. The deposited TiO₂ NP thin films on glass substrate were evaluated based on a water contact angle and sheet resistance. It was noted that the improvement the electrical conductivity and the hydrophilic properties of TiO₂ NP thin film were confirmed by increasing annealed temperature.

In summation, inkjet printing and screen printing processes could achieved the TiO₂ thin film thickness on an ITO glass at 10 μm and 17 μm respectively. The latter

showed the optimum conversion efficiency of DSSC at 8.75% by a single-layer printing and 9.2% by a double-layers printing. 3D printing was an alternative technique to fabricate the TiO_2 thin film. The nozzle distance was an important printing parameter to affect the surface attributes. It was reported that the nozzle distance between 1.5-2.5 mm gave the optimum micro quality of TiO_2 printed image.



CHAPTER 3

METHODOLOGY

3.1 Equipment and chemicals

3.1.1 Experimental equipment

1. 123D Design software
2. Computer Notebook DELL
3. Conditioning Mixer Machine AR -250.
4. Conductive glass (Fluorine-doped Tin Oxide : FTO) 4 mm thickness, Resistivity 11ohm/square, produced by Nippon Sheet Glass Co.,Ltd
5. Digital Hot plate HP-2LA
6. Multimeter for electrical measurement CD731
7. Tape 3M
8. Heat furnace KDF S-70
9. Ion coater Eiko IB.3
10. 3D Measureing Laser Microscope OLS500 LEXT Olympus
11. SourceMeter Model 2450 for sheet resistance measurement
12. Solar Simulator YS MASHITA DENSO
13. Rheometer gemini 200 hr nano
14. Scanning Electron Microscope QUANTA 450



Conditioning mixer AR -250



Rheometer gemini 200 hr nano



Digital Hot plate HP-2LA



Heat furnace KDF S-70



ion coater Eiko IB.3



Source Meter Model 2450



Scanning Electron Microscope QUANTA 450



Solar Simulator Yamashita Denso

Figure 3. 1 Equipment used in experiment

3.1.2 Chemicals

1. Nano Titanium dioxide paste (PST-18 NR) from JGJ Catalysts and Chemicals Ltd.
2. Organic dye (D205)
3. Acetonitrile, Super dehydrate
4. t-Butyl Alcohol (2-Methyl-2-propanol)
5. Chenodeoxycholic Acid
6. Ethanol (99.9%)
7. Iodide electrolyte (I_3^-)



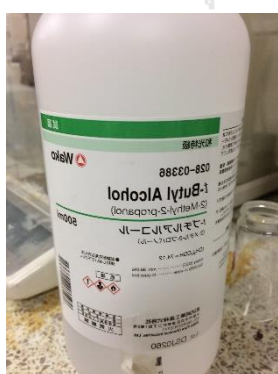
Nano Titanium dioxide paste
dehydrate



Organic dye (D205)



Acetonitrile, Super



t-Butyl Alcohol (2-Methyl-2-propanol)



Chenodeoxycholic Acid

Figure 3. 2 Chemicals used in experiment

3.2 Procedures

3.2.1 LDM 3D printer Assembly

The LDM 3D printer assembly was done in a fixed frame with the size of 400 x 350 x 600 mm³. The following components were fixed as shown in Fig. 3.3:

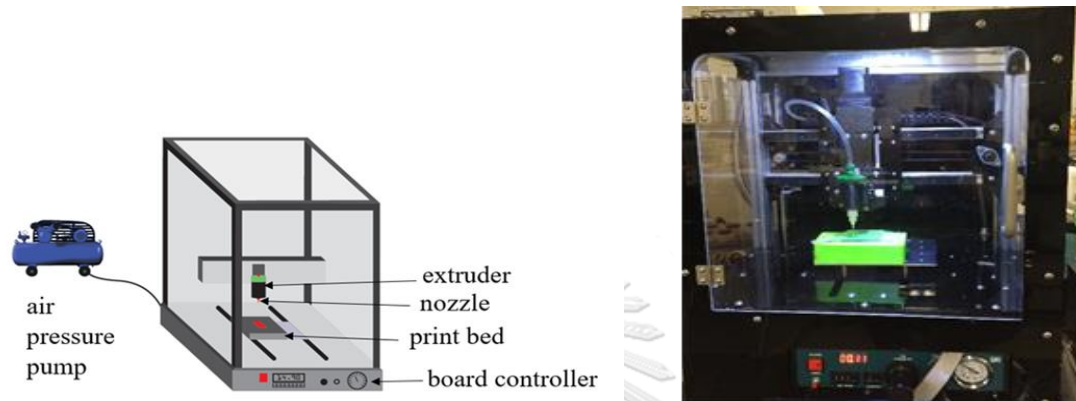


Figure 3. 3 LDM-type 3D printer.

- Print bed: the flat surface where the 3D models were layered during printing.
- Extruder: it was incorporated with a pump (air pressure) to push the TiO₂ paste through it. In this case, a syringe was chosen as an extruder.
- Extrusion tip or nozzle where the paste was fed though to deposit over the print bed. The nozzle size was varied in 0.42, 0.53, 0.63 and 0.70 mm as shown in Figure 3.4. The smaller the nozzle becomes, the higher the resolution of the print is.



Figure 3. 4 Nozzles size 0.42, 0.53, 0.63 and 0.70 mm

- Board controller: the main board which connects with the computer and all components including pump and motor.

- Air pressure pump: the device which emits air pressure to control the function of extruder

3.2.2 Preparation of TiO₂ paste

A mixture of Nano-titanium dioxide samples were prepared by mixing a PST-18NR Nano-Titanium Dioxide paste with 99.5% ethanol in a ratio of 10:1, 6:1 and 4:1; and then blended with centrifugal conditioning mixer AR -250.

3.2.3 Rheology measurement

The rotational Rheology type (controlled-stress) was chosen to measure the rheology property of each paste sample. The viscosity-stress curves were obtained. The measurement was done at temperature 25° C, using a gap size of 1000 μm. Each sample was measured three times. The averaged data was calculated.

3.2.4 Printing test

A 3D square file sized 5 x 5 mm and 0.0025 mm in height was designed by a computer Notebook using a 123D Design software as shown in Figure 3.5.

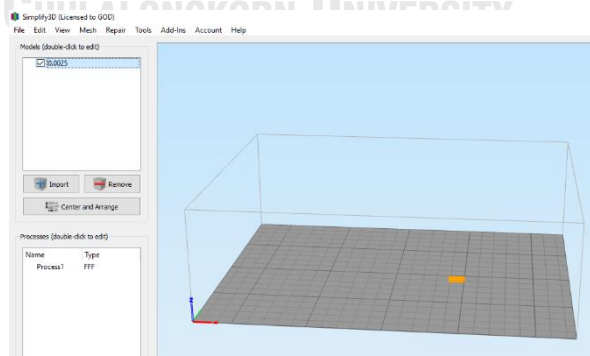


Figure 3. 5 A 3D square image size 5x5 and 0.0025 height

The 3D printer was set-up to fabricate the TiO₂ thin films. The effect of printer parameters such as printing speed, air pressure and nozzle size on the quality of the printed TiO₂ layer on the electrode glass was investigated.

The nozzle size 0.42, 0.53, 0.63 and 0.70 mm. were tested. Firstly, the printer was set-up as follows: the distance between the electrode plate and the nozzle tip was at 0.1 mm, air pressure at 3 bar, printing speed at 5 mm per second. Then, the TiO₂ paste was extruded on the Fluorine-doped tin oxide glass using the varied nozzle sizes. The printed TiO₂ samples were placed on a hot plate at 120 °C for 3 minutes and then put to a furnace at 500 °C for 4 hours. The crack-free fabricated layer was determined through optical microscope.

Using the proper nozzle size, the effect of air pressure and printing speed was continued. Firstly the air pressure at 2, 3, 4, 5 and 6 bar were varied with the fixed printing speed at 5 mm per second. Then, the printing speeds were changed at 15, 25, and 35 mm per second respectively. The fabricating test was done using the chosen air pressure from prior testing. The printed TiO₂ samples were obtained and placed on a hot plate at 120 °C for 3 minutes and then bringing to furnace at 500°C for 4 hours.

To determine the distance between the electrode plate and the nozzle tip, the distance was adjusted at 0.1, 0.2, 0.3, and 0.4 mm. The test was done using the proper printer parameters. The uniformity and crack-free on dried thin films were determine.

3.2.5 Design of thin films

Multiple printing was tested. 1-4 layers consecutive printing was proposed as shown in Figure 3.6 to find out the optimum layers to achieve the crack-free thin film, satisfied electrical sheet resistance and high conversion efficiency of DSSC.

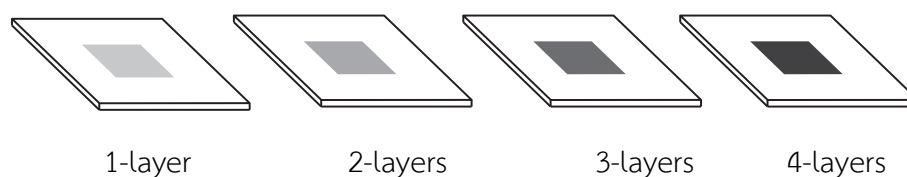


Figure 3. 6 Printed TiO₂ on electrode plates with different thickness from 1-4 layers

Based on prior experiment, pattern of printed films was designed into 3 types as follows: Disconnected patterns, Text and Different levelling patterns (connected patterns) as shown in Figure 3.7. Conversion efficiency of these obtained DSSC samples was measured.

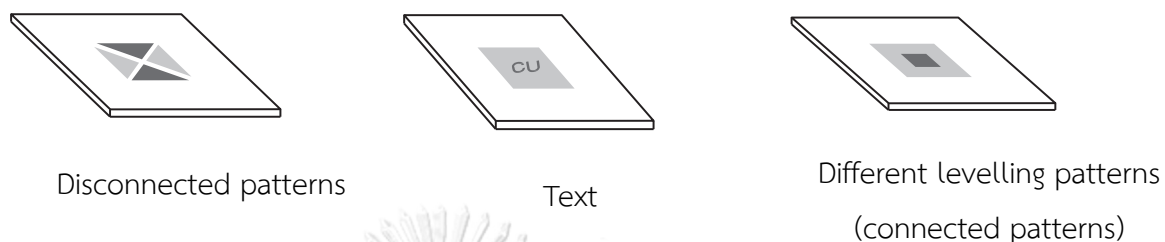


Figure 3. 7 Different patterns of printed TiO_2 thin films

3.2.6 DSSC assembly

3.2.6.1. Dye-sensitized solution was prepared by mixing 0.0087 g of dye (D 205), 0.00080 g of chenodeoxycholic acid, 25 ml acetonitrile super dehydrate and 25 ml t-butyl alcohol (2-Methyl-2-propanol). This type of dye was a standard dye commonly used in DSSCs. We can buy it in the chemical market.



Figure 3. 8 Dye-sensitized solution

3.2.6.2 The glass electrodes with TiO_2 thin film were Immersed into the dye solution as shown in Figure 3.9. The beaker was closed with rubber, wrapped in foil and stored in a dark place for 4 hours.

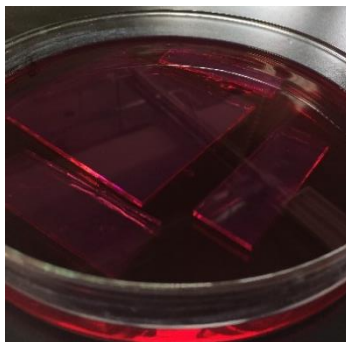


Figure 3. 9 The printed TiO₂ was immersed in the dye-sensitized solution

3.2.6.3. Counter electrode was prepared by coating platinum onto the glass using an ion coater with 4 mA current. A hole was drilled on the electrode.

3.2.6.4 The working electrode or printed TiO₂ plate was laminated on the counter-electrode plate using tape with electrolyte solution filled between them.

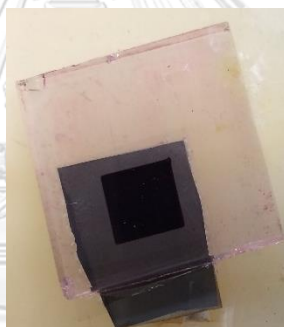


Figure 3. 10 A working electrode plate placed onto the counter-electrode plate

3.2.7 Thin film characteristic analysis

The printed TiO₂ thin films were characterized by measuring thickness, roughness, sheet resistance, uniformity and crack observation.

Scanning Electron Microscope (SEM) was used to evaluate the thickness, uniformity and crack of printed thin film samples. In addition the crack occurrence would be re-confirmed by using optical microscope. The roughness was printed thin films was measured by a 3D laser microscope. To evaluate the optimum of multilayer, we observed the crack occurrence on the printed thin films.

Sheet resistance of crack-free thin films were measured by using a 4-probe type SourceMeter Model 2450. The measurement was done 3 times with different positions. The averaged values were calculated.

To determine the efficiency of DSSC solar cell from different layers and patterns, the Conversion Efficiency of each printed samples were measured by using a Solar Simulator Yamashita Denso. The Xenon lamp power supply was adjusted by 100% intensity and 15 A current.



Chapter 4

Results

4.1 Rheology property of nano titanium dioxide paste

Result showed viscosity-shear rate dependence of TiO_2 paste at varying ratio of ethanol solution as shown in Figure 4.1 based on parallel plate geometry with varying control speed range from 0.01 milli rad/sec to 500 rad/s. The decrease in viscosity as shear rate increased indicated shear rate thinning behavior. This is typical of paste with high solid content system. The higher the solid content is, the stronger the change of viscosity becomes. Similar manners were also found by using other geometries. The measurement suggested that the paste has visco-elastic property. The behavior thus shall relate to printing condition such as printing speed and air pressure. To continue our experiment, we chose the TiO_2 paste sample at the ratio 10:1 w/w.

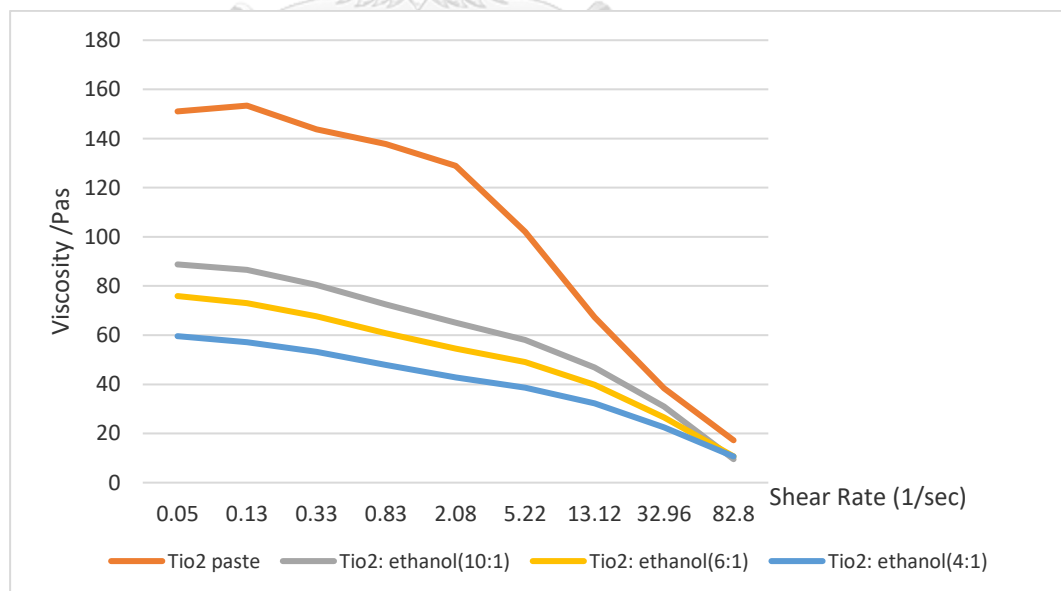


Figure 4. 1 Rheology property of TiO_2 paste samples (Viscosity vs Shear rate)

4.2 Printing test

4.2.1 Effect of nozzle size

It was found that the nozzle size of 0.42 and 0.53 mm gave the printed thin films without crack as shown in Figure 4.1. The bigger size of nozzle tended to create crack films as shown in Figure 4.2.

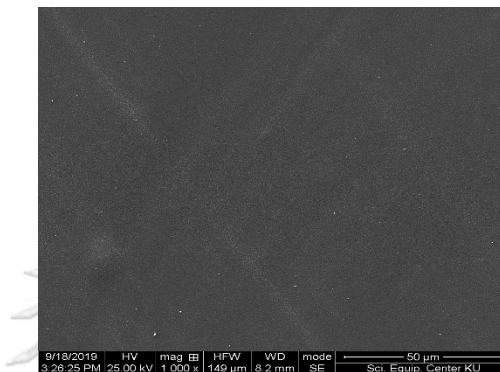


Figure 4. 2 Crack-free printed TiO_2 thin film on conductive glass using 0.42 nozzle size. (M x1000)

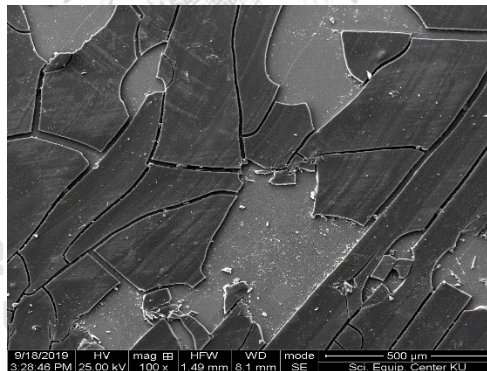


Figure 4. 3 SEM image of crack printed TiO_2 thin film using nozzle size 0.63 mm. (M x100)

4.2.2 Effect of printing speed, air pressure parameter and nozzle size

The relationship between nozzle sizes and air pressure was shown in Table 4.1 and 4.2. It was found that the lower air pressure of the 3D printer tended to create non-uniform TiO_2 printed thin films, while the higher air pressure accelerated the crack occurrence of thin films. Using nozzle size 0.42 mm, the proper air pressure was shown at 4 bar as there was no crack occurred. The observation was done by

optical microscope. If we used the bigger nozzle size, we had to compensate the extruded force by lowering the air pressure to 3 bar. Note that this range of printing speed (5-35 mm/sec) did not influence the quality of printed thin films.

Accordingly, It can be said that force and the amount of extruded TiO_2 paste are important factors to achieve the uniformity and crack-free thin films. Force depends on the combination of air pressure, printing speed and nozzle size. Higher force results in higher amount of extruded TiO_2 which can create cracking of the thin films. Thus, adjusting the printer's parameters is necessary to control extruding force and the amount of extruded TiO_2 paste from the syringe. In this experiment, the range of printing speed setting was in the save zone. This meant that this range (5 – 35 mm/sec) could not affect the increase of force to extrude the paste. It was found that the crack of thin films could be occurred at the printing speed over 50 mm/sec.

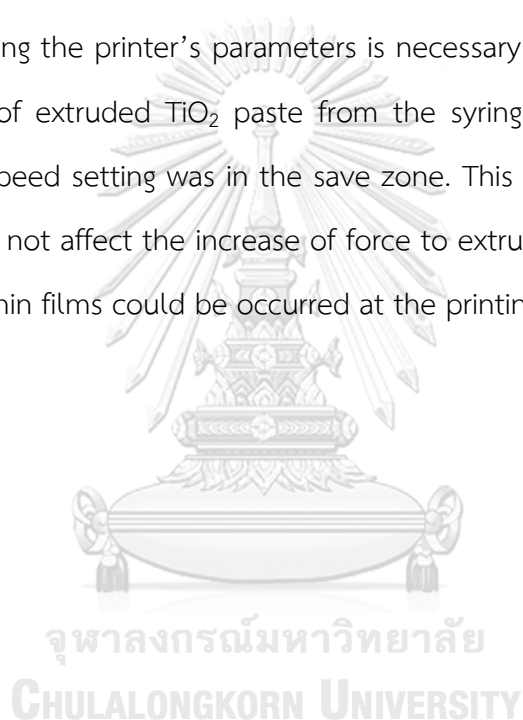


Table 4. 1 Enlarged images of printed TiO_2 thin films by varying air pressure and printing speeds, using nozzle size 0.42 mm





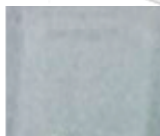





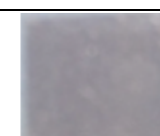
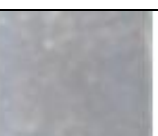


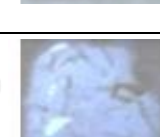


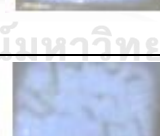















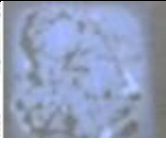



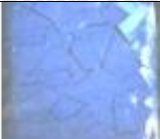

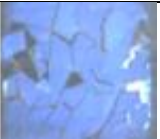
	Printing speed 5 mm/sec	Printing speed 15 mm/sec	Printing speed 25 mm/sec	Printing speed 35 mm/sec
Air pressure 2 bar				
Air pressure 3 bar				
Air pressure 4 bar				
Air pressure 5 bar				
Air pressure 6 bar				

Table 4. 2 Enlarged images of printed TiO₂ thin films by varying air pressure and printing speeds, using nozzle size 0.53 mm

	Printing speed 5 mm/sec	Printing speed 15 mm/sec	Printing speed 25 mm/sec	Printing speed 35 mm/sec
Air pressure 2 bar				
Air pressure 3 bar				
Air pressure 4 bar				
Air pressure 5 bar				
Air pressure 6 bar				

4.2.3 Effect of the distance between nozzle tip and electrode surface

Figure 4.4 shows SEM images of printed TiO₂ thin film at Magnification 2000 using nozzle 0.42 mm, air pressure 4 bar and printing speed 25 mm/sec. The distance between the nozzle tip and electrode surface was adjusted at 1 mm. The obtained thickness of thin film was at 5.561 μm .

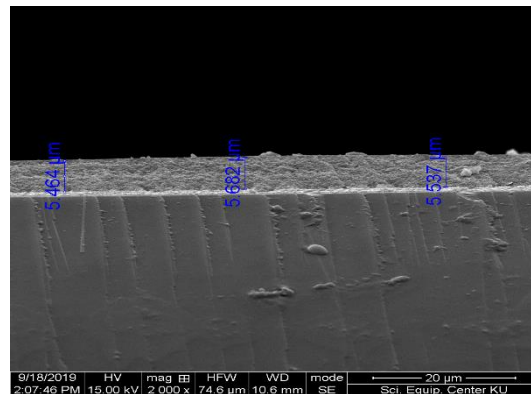


Figure 4. 4 SEM image of printed TiO₂ film by adjusting the distance between the nozzle tip and electrode surface at 1 mm (using nozzle size 0.42 mm)

It was found that when the distance was up to 2 and 3 mm, the thickness of thin films would decreased to be 5.432 μm and 4.249 μ respectively as shown in Figure 4.5.

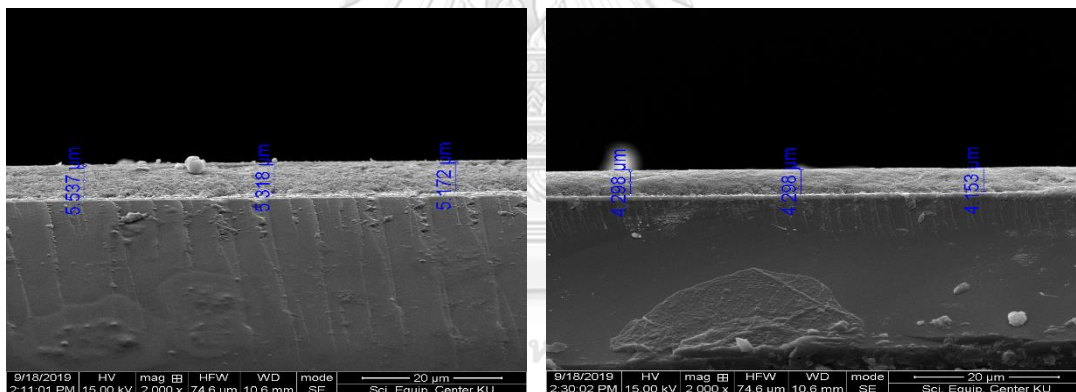


Figure 4. 5 SEM images of printed TiO₂ thin films adjusting the printing distance at 2 (left) and 3 mm (right) using nozzle size 0.42 mm

Figure 4.6 shows SEM image of thin film using nozzle size at 0.53 mm (air pressure 3 bar, printing speed 15 mm/sec). The printing distance (between the nozzle tip and electrode surface) was at 1 mm. The obtained thickness of printed TiO₂ thin film was 6.653 μm. It could be explained that the amount of extruded TiO₂ paste was increased even the force compensation was done.

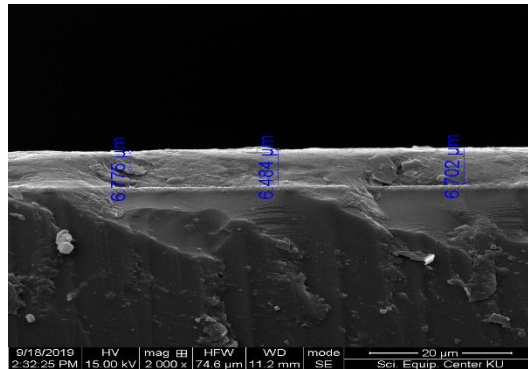


Figure 4. 6 SEM image of printed TiO_2 film by adjusting the distance between the nozzle tip and electrode surface at 1 mm (using nozzle size 0.53 mm)

Figure 4.7 shows the SEM images of printed thin films adjusting the printing distance at 2 and 3 mm. It was found that the thickness of thin films was decreased to be 6.143 μm and 5.245 μm respectively. However, in overall, the obtained thickness of thin film samples from 1-layer printing did not vary significantly. The average thickness value was at 5.547 μm .

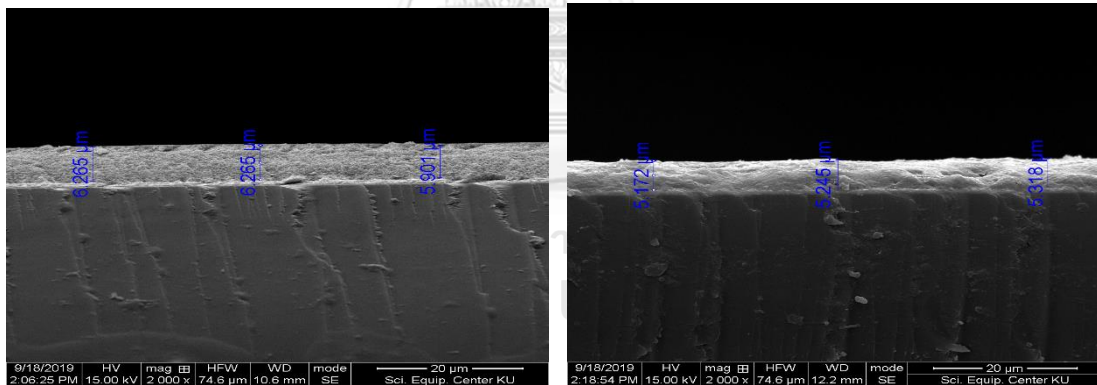


Figure 4. 7 SEM images of printed TiO_2 thin films adjusting the printing distance at 2 (left) and 3 mm (right) using nozzle size 0.53 mm

4.3 sheet resistance of thin film

Figure 4.8 shows the sheet resistance curves of printed TiO_2 thin films using nozzle size 0.42 / 0.53 mm and printing distance at 1 mm. The sheet resistance values were plotted by varying the printing speed from 5 to 35 mm/sec. Results

show the range of sheet resistance values between 5.10 – 6.99 M Ω /Sq using nozzle size 0.42 mm + air pressure 4 bar. While the range between 5.77 – 9.37 M Ω /Sq fell in the printing condition using nozzle size 0.53 mm + air pressure 3 bar. Thus, it could be said that the printing condition using small nozzle with proper printing speed gave preferable conductivity. Sheet resistance was varied depending on the quality of printed thin films such as uniformity, roughness and crack. Higher amount of extruded TiO₂ tended to lower the quality of printed thin films by which the relevant sheet resistance was increased. This implies that achieving optimum quality of printed TiO₂ thin films need proper extruded force and amount of extruded TiO₂ paste. Form this experiment, it was suggested that the suitable setting of printer's parameters for TiO₂ fabrication recommended nozzle size 0.42 mm, air pressure 4 bar, printing speed 25 mm/sec and printing distance 1 mm as it gave crack-free thin film with lowest sheet resistance.

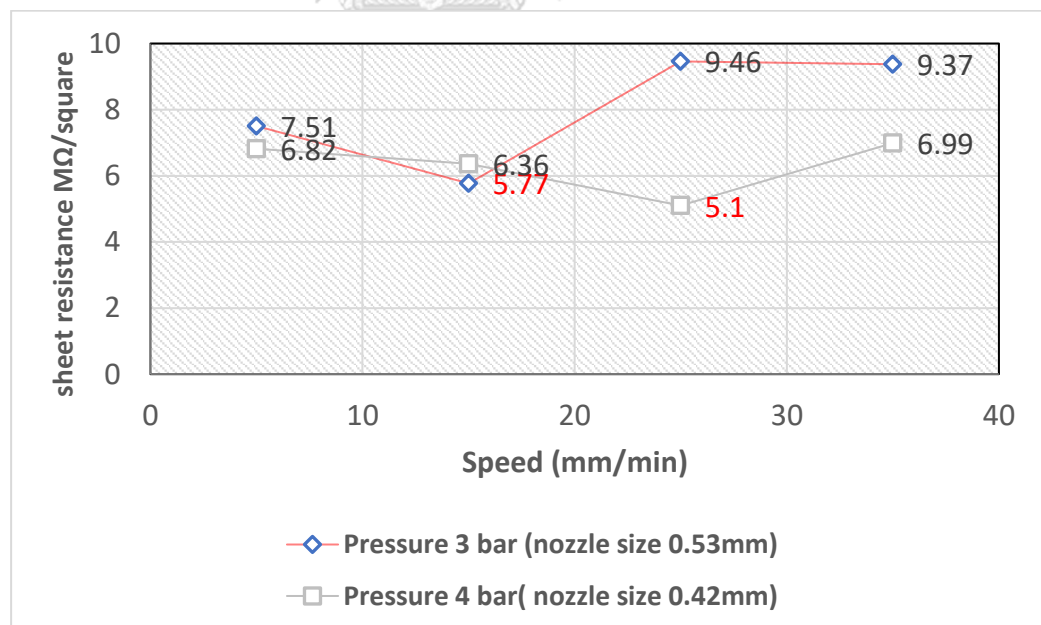


Figure 4. 8 Sheet resistance curves of printed thin films, using nozzle size 0.42 mm and 0.53 mm

4.4 Thin film characteristics

The uniformity and surface roughness of printed TiO₂ thin film was analyzed by 3D measuring laser microscope. Figure 4.9 revealed the measured surface profile representing its uniformity with Ra roughness at 0.482 μm and 0.703 μ for nozzle size 0.42 mm and 0.53 mm respectively. Smaller nozzle size gave better uniformity with lower surface roughness.

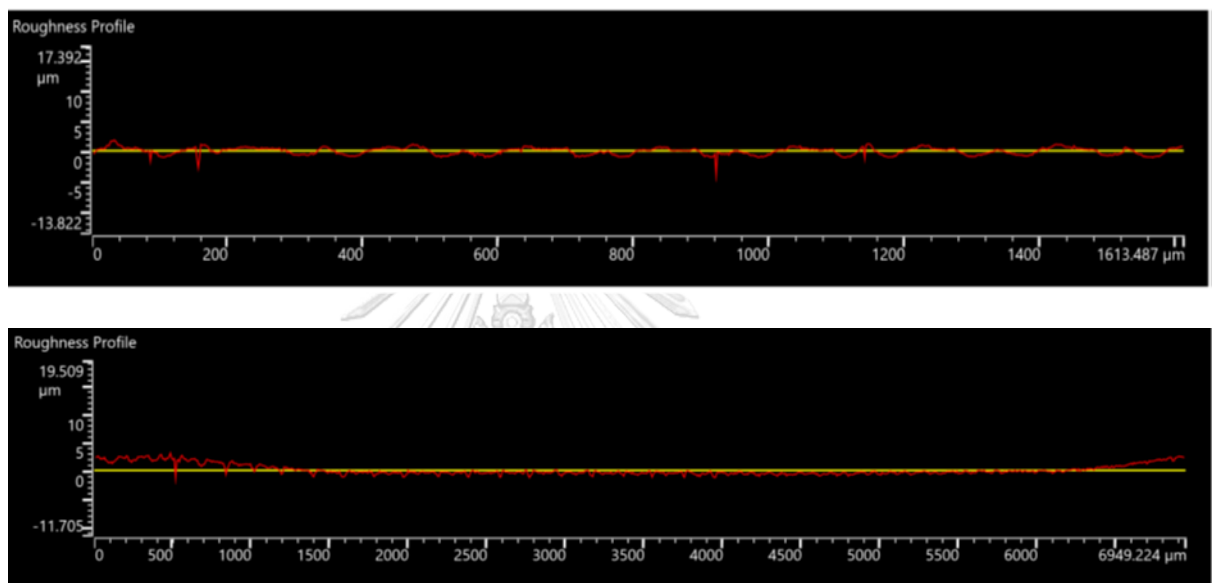


Figure 4. 9 Surface profile of printed TiO₂ thin films using nozzle size 0.42 (above) and 0.53 mm (below) (1 layer)

4.5 Multi-layer printing

The printed TiO₂ thin film samples with varying the number of layer were analyzed by SEM and eye observation. SEM Images of cross section of thin films are shown in Figure 4.10. It was found that the thickness of printed thin films was increased relevant to the number of layer. Spreading phenomenon of wet TiO₂ paste during multi-printing was occurred. Accordingly, the increased thickness of thin films was not high as expected. It was found that the crack-free thin films could be achieved by three-layer printing. For four-layer printing, it gave the printed TiO₂ thin

films with crack. It could be seen by naked eyes. It was confirmed by sheet resistance values. Table 4.3 shows the results of thickness of sheet resistance of printed TiO₂ thin films by multi-printing using nozzle size 0.42 mm + printing speed 25 mm/sec.

Table 4. 3 Thickness and sheet resistance of printed TiO₂ thin films by multi-printing

Number of layer	Thickness (μm)	Sheet resistance ($\text{M}\Omega/\text{Sq}$)
1	5.56	5.10
2	5.88	6.45
3	6.25	6.81
4	6.38	167.07 (crack)

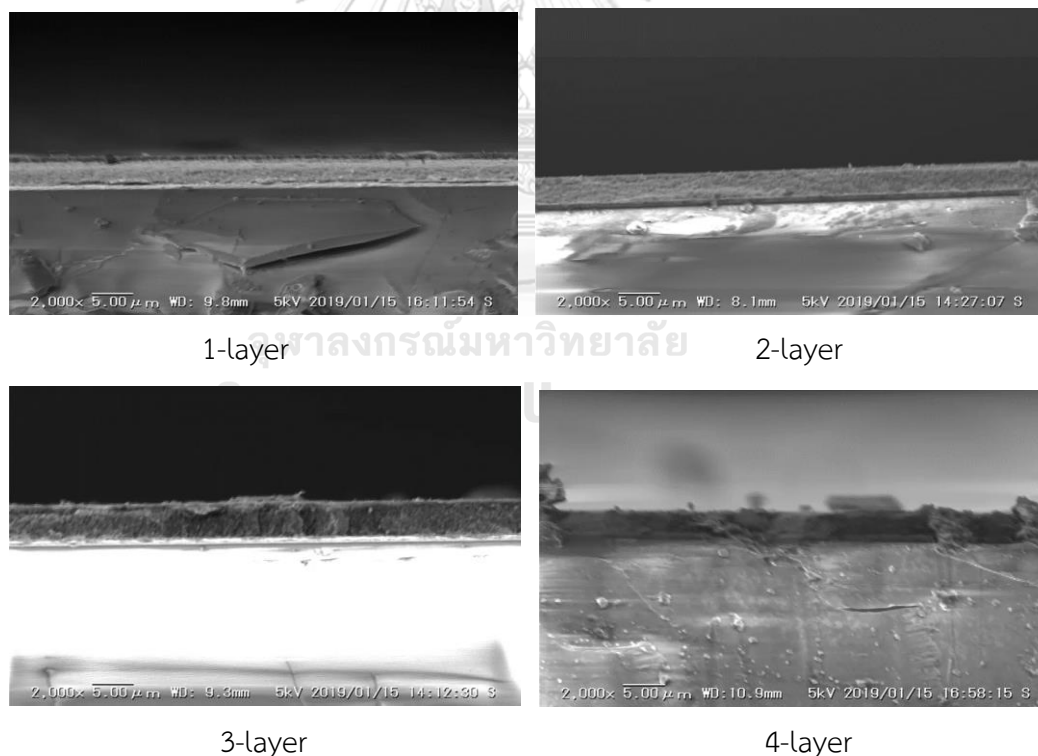


Figure 4. 10 SEM Images of cross section of printed TiO₂ thin films (Mx2000)

4.6 Conversion efficiency of DSSC

The conversion efficiency values of DSSCs by multi-layer printing are given in Table 4.4. The samples were related to the results of printed thin films from Table 4.3. It was found that the obtained values from 1-3 thin film layers were not significantly different as they were in the range of 4.10 ± 0.05 %. This implied that the conversion efficiency of DSSCs did not relate to the thickness of TiO_2 thin films, even the sheet resistance of each electrode were varied. They depend on the chemical components used in the DSSC such as dye types. This value is not too low and not too high. It is confirmed that the application of 3D printer to fabricate the DSSC is possible to achieve the acceptable conversion efficiency values.


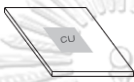

Table 4. 4 Conversion efficiency values of DSSCs by multi-layer printing

Number of printed layer	Jsc (mA/cm ²)	Voc (mV)	FF	η (%)
1	10.4	699	0.56	4.07
2	10.8	674	0.56	4.08
3	10.2	699	0.58	4.14
4	-	-	-	Crack

FF: Field factor (The ratio of max obtainable power to the product of the open-circuit voltage and short-circuit current)

For the DSSCs with designed patterns, the measured conversion efficiency values tended to decrease as given in Table 4.5. The variable patterns of printed thin films did not affect the change of the values. The range of conversion efficiency values was in the range of 3.10 ± 0.10 %. Interestingly, the obtained values could be applied for optoelectronic devices. It is suggested that the improvement should be done by chemical change.

Table 4. 5 Conversion efficiency values of DSSCs with different patterns of printed thin films

Pattern types	Image design	Jsc (mA/cm ²)	Voc (mV)	FF	η (%)
Disconnected patterns		8.81	759	0.45	3.01
Text		9.48	743	0.42	2.96
Different levelling patterns (connected patterns)		9.31	694	0.50	3.23

Chapter 5

Conclusion and Discussion

In the study, I focused on the rheology property of nano titanium dioxide paste and the effect of 3D printer's parameters such as nozzle size, air pressure, printing speed and the distance between nozzle tip and electrode surface on the quality of TiO₂ thin film and electrical conductivity, the conclusions could be listed as follows:

Result suggested that using the small nozzle size at 0.42 mm was preferable, however, it was possible to use the nozzle size both 0.42 and 0.53 mm to give the printed thin films without crack. The increase of nozzle size shall be compensated by lower air pressure. For example, using nozzle size 0.42 mm, with printing distance at 1 mm and printing speed 5-35 mm/min, the proper air pressure was set at 4 bar to obtain crack-free thin films. While using the bigger nozzle size 0.53 mm with the same printing condition, the air pressure would be lowered to 3 bar to achieve the same quality of thin films. Note that printing speed setting from 5 to 35 mm/sec was in the save zone as this range did not affect much the quality of thin films. Higher printing speed over this limit must be compensated by lower air pressure or bigger nozzle size.

The closer printing distance between the nozzle tip and the surface of substrate was preferred. Accordingly, the distance at 0.1 mm was suggested in this experiment. Higher distance gave less thin film's thickness and tended to occur non-uniformity of thin films.

Based on the mixing ratio TiO₂:ethanol 10:1, the printing test showed that the proper parameters setting of the LDM 3D printer would be:

- nozzle size 0.42 mm,
- printing distance at 0.1 mm,
- air pressure 4 bar
- printing speed 5 - 35mm/sec.

This printing condition gave crack-free thin films with average thickness about 5.5 μm and related sheet resistance in the range of 5.1 – 6.9 $\text{M}\Omega/\text{Sq}$. It was found that at printing speed 25 mm/sec, the result of sheet resistance showed the lowest value at 5.10 $\text{M}\Omega/\text{Sq}$. While using nozzle size 0.53 mm, the obtained sheet resistance was in the range of 5.77 – 9.37 $\text{M}\Omega/\text{Sq}$.

By thin films characterization, it was found that smaller nozzle size such as 0.42 mm gave better uniformity with lower surface roughness.

For multiple printing, based on crack-free quality, the optimum number of printed layers would be 3 layers. The obtained thickness of thin films by 1-3 layers would not deviate much as the occurrence of spreading effect. The range of thickness was 5.5 – 6.25 μm . Interestingly, the conversion efficiency of DSSCs among 1-3 layer was acceptable at the value of about 4%. The values did not change as the chemical ingredients in the DSSC system were the same. In addition, it was found that the conversion efficiency of DSSCs among different patterns was still existed at the value of 3%.

In conclusion, a simple and cheap LDM 3D printer was demonstrated to fabricate the TiO_2 thin film by using the commercial TiO_2 paste available in the market. The limitation of this system resulted in three successive layers printing for TiO_2 thin film fabrication. The multi-layer did not significantly affect the increase of TiO_2 thin films. Instead, the spreading occurrence was appeared. The reason is that the extruded paste's viscosity is not high enough to support the body of thin films.

The ratio 10:1 thus may have to be re-adjusted in this case. In addition, the property of TiO_2 is needed to consider such as size and chemical structure. However, the advantage of 3D printing technique will open the new design and quality guarantee for the performance of DSSC.

The extrusion force of the 3D printer is the key factor to achieve the satisfied quality of TiO_2 thin film such as uniformity, thickness, roughness, crack-free and electrical conductivity. This force is resulted from the combination of the printer's parameters setting such as nozzle size, printing distance, air pressure and printing speed. It should be noted that after fabrication, the TiO_2 thin films must be baked at high temperature up to 500°C . By this system, the thin film's thickness or the amount of extruded TiO_2 paste shall be controlled to protect the cracking occurrence. Accordingly, the setting of printer's parameters is necessary by which the values must be related to the rheological property of the paste.

For further study, the application of LDM 3D printer can be expanded to print sensitized dyes on the printed TiO_2 thin films or even the fabrication of Pt on counter electrode. This will enhance the quick and controllable process to make the DSSC. It is hope that the use of 3D printer for DSSC will be another choice among DSSC experts worldwide as this type of printing technique has advantages over other printing techniques such as variable pattern design.

Another suggestion is the improvement of LDM 3D printer as this study is a prototype test using the easy assembled printer. The choice of nozzle size should have more selection on small size. The machine operation is still manual process. Thus, stable and automation machine should be reconsidered.

REFERENCES

1. Gross, B.C., et al., *Evaluation of 3D Printing and Its Potential Impact on Biotechnology and the Chemical Sciences*. Anal. Chem, 2014. **86**(7): p. 3240-3253.
2. Kop, R., et al. *Adjusting the Factory Planning Process when Using Immature Technologies*. in *Procedia CIRP*. 2016.
3. G, I., D. W.R, and B. S, *Additive Manufacturing Technologies*, ed. Springer. 2010.
4. A, Y., N. F, and I. K, *A three-dimensional microfabrication system for biodegradable polymers with high resolution and biocompatibility*. Journal of Micromechanics and Microengineerin, 2008. **18**(2): p. 25-35.
5. M, M., et al., *Process and material behavior modeling for a new design of micro-additive fused deposition*. International Journal of Advanced Manufacturing Technology, 2013. **7**: p. 9-12.
6. I, Z., et al., *Fused deposition modeling of novel scaffold architectures for tissue engineering applications*. Biomaterials, 2002. **23**(4): p. 1169-1185.
7. B, O.R. and G. M, *A low-cost, high-efficiency solar cell based on dyesensitized colloidal TiO₂ films*. Nature, 1991. **353**: p. 737-740.
8. D, F.R., C. K., and T. D, *Three-dimensional printing of freeform helical microstructures: a review*. Nanoscale, 2014. **18**(2): p. 10470-10485.
9. Yang, P., *Chemistry Of Nanostructured Materials volume II*, ed. W.S. Publishing.Co.Pte.Ltd. 1993, New Jersey, London, Singapore, Beijing, Shanghai, Hongkong, Taipei, Chennai
10. M, N., et al., *An analytical study of the porosity effect on dye-sensitized solar cell performance*. 90, 2006. **9**: p. 1311-1344.
11. D.G., L.N.S.N., *Powering the planet: Chemical challenges in solar energy utilization*. Proc. Natl. Acad. Sci. U.S.A., 2006. **103**(43): p. 15729-15735.
12. K, M., et al., *Solid-state dye-sensitized solar cells fabricated by coupling photoelectrochemically deposited poly(3,4-ethylenedioxythiophene) (PEDOT) with silver-paint on cathode*. J. of Chemical Communications, 2011. **47**(11): p.

- 3120-3125.
13. M.F, H., et al., *Influence of direct current power on the photocatalytic activity of facing target sputtered TiO₂ thin films*. J. of Thin Solid Films, 2008. **517**(3): p. 1091-1095.
 14. I, G., R. D.W., and S. B, *Additive manufacturing technologies – Rapid prototyping to direct digital manufacturing*, Springer, Editor. 2010.
 15. M, V. and Y. S, *Chapter 2: Freeform fabrication of nanobiomaterials using 3D printing*, Book entitled *Rapid prototyping of biomaterials*, ed. W.P. Limited. 2014, UK.
 16. S.J, L., et al., *A Simple, low-cost conductive composite material for 3D printing of electronic sensors*, . PLoS ONE, 2012. **7**(11): p. 49365
 17. S.Z, G., et al., *Solvent-cast three-dimensional printing of multifunctional microsystems*, *Small (Macro and Nano)*. Wiley Online Library, 2013. **9**(24): p. 4118-22.
 18. G, P., et al., *Conductive 3D microstructures by direct 3D printing of polymer/carbon nanotube nanocomposites via liquid deposition modeling*. J. of Composites: Part A,, 2015. **76**: p. 110-114.
 19. P, B., et al., *Novel electrochromic devices based on complementary nanocrystalline TiO₂ and WO₃ thin films*. J. of Thin Solid Films, 1999. **350**: p. 269.
 20. H, T. and H. P.T, *Solid-State Photovoltaic thin films using TiO₂, organic dyes and layer-by-layer polyelectrolyte nanocomposites*. J. of Adv. Functional Materials, 2003. **13**: p. 831-839.
 21. Z, C., et al., *Photocatalytic activity enhancement of Anatase TiO₂ by using TiO*. J. of Nanomaterials., 2014. **9**.
 22. A, D.P., B. M, and P. L, *Brookite, the Least Known TiO₂ Photocatalyst*. J. of Catalysts 2013. **3**(1): p. 36-73.
 23. D, M., et al., *On the structural properties and optical transmittance of TiO₂ r.f. sputtered thin films*. J. of Applied Surface Science., 2000. **156**: p. 200-206.
 24. D, M., et al., *Chromium-doped titanium oxide thin films*. J. of Material Science and Engineer, 2005. **118**(1-3): p. 187-191.

25. M, G., *Photoelectrochemical cells*. Nature 2001. **414**: p. 338-344.
26. M., A., M. Y, and Y. S, *Formation of titania nanotubes with high photo-catalytic activity*. J. of Chemical Communications, 2000. **8**: p. 942-943.
27. M.S.P, S., et al. *Crack-Free TiO₂ Thin Film via Sol-Gel Dip Coating Method: Investigation on Molarity Effect*. in *Proc. of IOP Conf. Series: Materials Science and Engineering*,. 2018.
28. J, D.G.B. and S.U. S, *Inkjet printing of polymer micro-arrays and libraries: Instrumentation, requirements, and perspectives*. J. Macromolecular Rapid Communications, 2003. **24**: p. 659-666.
29. K.K.B., H., L. L., and H.I. M, *Direct writing technology-Advances and developments*. Cirp Annals-Manufacturing Technology, 2008. **57**: p. 601-620.
30. T.K, G., et al. *Screen-printed dye-sensitized large area nanocrystalline solar cell*. in *Material Research Society Symposium Proceedings*. 2000.
31. D, Z., et al., *Nanocrystalline TiO₂ electrodes prepared by water-medium screen printing technique*. J. Chemistry Letters, 2001. **30**: p. 1042-1043.
32. T, M., et al., *Preparation and properties of nanostructured TiO₂ electrode by a polymer organic-medium screen-printing technique*. J. Electrochemistry Communications., 2003. **5**: p. 369-372.
33. P, G. and M. M, *The relation between TiO₂ nano-pastes rheology and dye sensitized solar cell photoanode efficiency*. J. Materials Science in Semiconductor Processing, 2015. **30**: p. 605-611.
34. I, S., et al., *Fabrication of Screen-Printing Pastes From TiO₂ Powders for Dye-Sensitized Solar Cells*. J. Progress in Photovoltaics: Research and Applications, 2007. **15**: p. 603-612.
35. G, R., C. P, and G.M. A, *Contribution to the optical design of dye-sensitized nanocrystalline solar cells*. J. Solar Energy Materials and Solar Cells, 1999. **58**: p. 321-336.
36. W.Y, P.-H., et al., *Stable inks for inkjet printing of TiO₂ thin films*. J. Materials Science in Semiconductor Processing, 2018. **81**: p. 75-81.
37. R, C., et al., *Inkjet-printed TiO₂ nanoparticles from aqueous solutions for dye-sensitized solar cells (DSSCs)*. J. Energy Technol, 2015. **3**: p. 866-870.

38. M, A., et al., *Deposition of photocatalytically active TiO₂ films by inkjet printing of TiO₂ nanoparticle suspensions obtained from microwave-assisted hydrothermal synthesis*. J. Nanotechnology, 2012. **23**: p. 165603.
39. al, H.A.e., *Material development for dye solar modules: results from an integrated approach*. J. Prog. Photovolt.: Res Appl., 2008. **16**: p. 489-501.
40. al, H.A.e., *Dye solar modules for façade applications: recent results from project colorsol Sol*. J. Energy Mater. Sol. Cells., 2009. **93**: p. 820-824.
41. Lewis, J.A. and G.M. Gratson, *Direct writing in three dimensions*. J. Materials Today, 2004. **7**: p. 32-39.
42. Ahn, S.H., et al., *Measurement of anisotropic compressive strength of rapid prototyping parts*. J. Materials Processing Technology, 2007. **187-188**: p. 627-630.
43. Rimell, J.T. and P.M. Marquis, *Selective laser sintering of ultra high molecular weight polyethylene for clinical applications*. J. Biomedical Materials Research, 2000. **53**: p. 414-420.
44. M, S., P. D, and R. T, *Selective laser sintering of PEEK*. J. Cirp Annals-Manufacturing Technology, 2007. **56**: p. 205-208.
45. Zhuo, X., et al., *Fabrication of porous scaffolds for bone tissue engineering via low-temperature deposition*. J. Scripta Materialia, 2002. **46**: p. 771-776.
46. Vozzi, G., et al., *Microfabricated PLGA scaffolds: A comparative study for application to tissue engineering*. J. Materials Science and Engineering, 2002. **20**: p. 43-47.
47. T, H., *Reaction of Excited Chlorophyll Molecules at Electrodes and in Photosynthesis*. J. Photochemistry and Photobiology, 1972. **16**(4): p. 261-269.
48. V, N., et al., *Very efficient visible light energy harvesting and conversion by spectral sensitization of high surface area polycrystalline titanium dioxide films*. J. Am. Chem. Soc, 1988. **110**(4): p. 1216-1220.
49. B, O.R. and G. M, *High-Efficiency Solar Cell Based on Dye Sensitized Colloidal TiO₂ Films*. Nature, 1991. **353**: p. 737-740.
50. C, C.-Y., et al., *Highly Efficient Light- Harvesting Ruthenium Sensitizer for Thin-Film Dye-Sensitized Solar Cells*. ACS Nano, 2009. **3**(10): p. 3103-3109.

51. Chiba, Y., et al., *Dye-Sensitized Solar Cells with Conversion Efficiency of 11.1%*. Jpn. J. Appl. Phys, 2006. **45**: p. 638.
52. Y, A., et al., *Porphyrin-Sensitized Solar Cells with Cobalt (II/III)-Based Redox Electrolyte Exceed 12 Percent Efficiency*. Science, 2011. **334**(6056): p. 629-634.
53. Grätzel, M., *The Advent of Mesoscopic Injection Solar Cells*. Progress in Photovoltaics: Research and Applications, 2006. **14**(5): p. 429-442.
54. C, X. and S. S, *Titanium Dioxide Nanomaterials: Synthesis, Properties, Modifications, and Applications*. Chemical Reviews, 2007. **107**(7): p. 2891-2959.
55. P, N.-G., J.v.d. L, and A.J. F, *Comparison of Dye-Sensitized Rutile- and Anatase-Based TiO₂ Solar Cells*. The Journal of Physical Chemistry B,, 2000. **104**(38): p. 8989-8994.
56. J.B, C., et al., *Nanocrystalline Titanium Oxide Electrodes for Photovoltaic Applications*. Journal of the American Ceramic Society, 1997. **80**(12): p. 3157-3171.
57. K, N. and L. H, *Measuring methods of cell performance of dye-sensitized solar cells*. Review of Scientific Instruments, 2004. **75**(9): p. 282-283.
58. L, Y., C.-Y. H, and C.-L. T, *printing technology for dye-sensitized solar cells*. Advanced Materials Research, 2012. **476-478**: p. 1767-1770.
59. Z.i, Y., W. H, and C. G, *Effects of nozzle distance on micro quality in 3D printing*. Applied Mechanics and Materials, 2014. **644-650**: p. 4900-4904.
60. P, C. and S. K, *The Improvement of the Efficiency of Dye Sensitized Solar Cells by TiO₂ Blocking Layer*. J. SDU Res,, 2016. **9**(2): p. 120-140.
61. H, S.G., et al., *Dye-sensitized solar cells with inkjet-printed dyes*. Energy & Environmental Science, 2016. **9**: p. 2453-2462.
62. Y, C.-L., *TiO₂ thick film printing paste for dye sensitized solar cell*, in *Department of material Science and Engineering*. 2011, CASE WESTERN RESERVE University.
63. K, M.I., *The Optimization of Dye-Sensitized Solar Cells in Department of Electrical Engineering*,. 2017, University of South Florida.
64. S, S., *The fabrication of DSSC using natural dyes extracted from stem bark*, in *Department of Science Education*. 2014, kanchanaburi rajabhat university.

65. T, B., *The effect of annessling temperature on electrical sheet resistance and water contact angle of TiO₂ nanoparticle thin films prepared by sparking process*, in *Physic and general science program, Faculty of science and technology*. 2016, Nakhon ratchasima rajabhat university.





จุฬาลงกรณ์มหาวิทยาลัย
CHULALONGKORN UNIVERSITY

VITA

NAME Mr. Krairop Charoernsopa

DATE OF BIRTH 1 January 1982

PLACE OF BIRTH Bangkok

INSTITUTIONS ATTENDED Bachelor Degree of Science, Major in Printing Technology, Faculty of Industrial Education and Technology, King Mongkut's University of Technology Thonburi Fiscal Year 2004.

Master Degree of Science, Major in Imagine and Printing Technology, Faculty of Science, Chulalongkorn University Fiscal Year 2008

HOME ADDRESS 70 Soi Sirindhorn 7 Sirindhorn Road Bang Phlat Bangkok 10700.